

Authors are encouraged to submit new papers to INFORMS journals by means of a style file template, which includes the journal title. However, use of a template does not certify that the paper has been accepted for publication in the named journal. INFORMS journal templates are for the exclusive purpose of submitting to an INFORMS journal and should not be used to distribute the papers in print or online or to submit the papers to another publication.

Sample-Efficient Clustering and Conquer Procedures for Parallel Large-Scale Ranking and Selection

Zishi Zhang

Wuhan Institute of Artificial Intelligence, Guanghua School of Management, Peking University, Beijing, China;
Xiangjiang Laboratory, Changsha, China, zishizhang@stu.pku.edu.cn

Yijie Peng

Wuhan Institute of Artificial Intelligence, Guanghua School of Management, Peking University, Beijing, China;
Xiangjiang Laboratory, Changsha, China, pengyijie@gsm.pku.edu.cn

We propose novel “clustering and conquer” procedures for the parallel large-scale ranking and selection (R&S) problem, which leverage correlation information for clustering to break the bottleneck of sample efficiency. In parallel computing environments, correlation-based clustering can achieve an $\mathcal{O}(p)$ sample complexity reduction rate, which is the optimal reduction rate theoretically attainable. Our proposed framework is versatile, allowing for seamless integration of various prevalent R&S methods under both fixed-budget and fixed-precision paradigms. It can achieve improvements without the necessity of highly accurate correlation estimation and precise clustering. In large-scale AI applications such as neural architecture search, a screening-free version of our procedure surprisingly surpasses fully-sequential benchmarks in terms of sample efficiency. This suggests that leveraging valuable structural information, such as correlation, is a viable path to bypassing the traditional need for screening via pairwise comparison—a step previously deemed essential for high sample efficiency but problematic for parallelization. Additionally, we propose a parallel few-shot clustering algorithm tailored for large-scale problems.

Key words: simulation, ranking and selection, parallel computing

1. Introduction

Ranking and selection (R&S) aims to identify the best design from a finite set of alternatives, through conducting simulation and learning about their performances. In recent years, the large-

scale R&S problem, especially in the context of parallel computing environments, has emerged as an important research topic (Luo et al. 2015, Ni et al. 2017, Zhong and Hong 2022). Here, “large-scale” refers to a large number of alternatives, denoted by p . Most of the prominent existing large-scale R&S procedures are fully-sequential in nature, which are usually more sample-efficient due to the inclusion of screening steps based on pairwise comparisons. However, they encounter considerable hurdles in parallel implementation due to frequent information communication and synchronization issues (Luo et al. 2015, Ni et al. 2017). Recent advancements have focused on overcoming the limitations of the all pairwise comparison paradigm. For instance, Zhong and Hong (2022) propose a Knockout Tournament (KT) procedure to restrict comparisons to matches involving only two alternatives. Pei et al. (2022) compare each alternative against a common standard to avoid exhaustive pairwise comparisons. On the contrary, stage-wise methods, which predetermine the number of replications, are more naturally parallelizable. Nonetheless, a notable drawback of these methods is their typically high requirement for sample sizes.

To break this dilemma, we propose *parallel correlation-based clustering and conquer* (P3C) procedures, which leverage correlation information among alternatives for clustering to enhance sample efficiency. Existing R&S methods typically assume independence among alternatives and discard shared structural information (Eckman and Henderson 2022), with exceptions such as Fu et al. (2007), Qu et al. (2015), Li et al. (2022), Zhou et al. (2023). However, none of these existing methods that utilize shared information is tailored for large-scale problems, and they lack a rigorous mathematical analysis to elucidate and quantify the benefits derived from integrating similarity information, despite showing promising experimental results. Zhong and Hong (2022) point out that it is important to understand the growth rate of the required total sample size as p increases. Along this line, we prove that correlation-based clustering techniques in P3C can achieve an $\mathcal{O}(p)$ reduction in sample complexity, which is theoretically the optimal reduction rate.

Screening via frequent pairwise comparison is often considered to be the cornerstone for achieving high sample efficiency in R&S (Hunter and Nelson 2017), despite its difficulty in parallelization. In

this paper, valuable correlation information offers a new promising avenue: an experiment with 10^5 alternatives demonstrates that the screening-*free* version of P3C requires only 2% of the sample size compared to traditional stage-wise procedure (Rinott 1978) and even outperforms KT, one of the most sample-efficient screening-based procedures, by using only 60% of the sample size. To illustrate the motivation of P3C, we provide the following examples.

- **Drug discovery:** As depicted in Figure 1(a), the process of developing new drugs typically starts with a base molecule, followed by creating multiple variants through atom substitution (Negoescu et al. 2011). The Free-Wilson model (Free and Wilson 1964) describes a drug’s effect as the summation of the effects of each substitution atom: *the value of the drug = value of the base molecule + value of atom X + ...*. This can be viewed as a latent factor model, where the behavior of each atom is a random variable (latent factor). In large-scale scenarios, numerous drugs influenced by shared latent factors may exhibit significant correlation and show a clear clustering phenomenon (see Figure 4(b)).

- **Neural Architecture Search (NAS):** NAS, a key challenge in deep learning, aims to search for the best-performing neural architecture design. As depicted in Figure 1(b), the large search space is composed of combinations of multiple decisions, including the number of layers, the type of activation functions, the type of operations and so on. Nonetheless, evaluating and ranking architectures on test datasets is computationally intensive. To reduce the problem dimension, many state-of-the-art algorithms (Guo et al. 2020, Mellor et al. 2021) leverage the shared information among structurally similar architectures.

Motivated by the practical examples, the intuition behind P3C is to reduce the complexity of the problem by selecting a *representative* from a cluster of highly correlated alternatives. Note that, in this study, the correlation between alternatives serves as a general measure of inherent similarity, arising from various shared latent factors, not limited to common random numbers (CRN). P3C can be seen as a variant of the “divide and conquer” strategy in parallel R&S (Ni et al. 2017, Zhong and Hong 2022). It clusters alternatives based on correlations, assigns each cluster to a

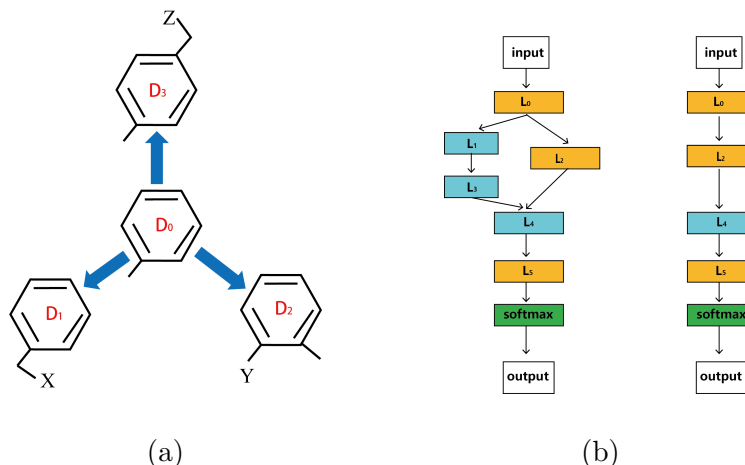


Figure 1 (a) Drug Discovery. (b) Neural Architecture Search.

single processor, and then selects a *representative* local best from each cluster for final comparison. A related study by Li et al. (2022) uses Gaussian Mixture Models (GMM), a clustering algorithm based on mean performance, to extract shared information in *non-parallel* settings. However, in parallel R&S, clustering alternatives with similar mean performance on the same processor can be detrimental due to the increased challenge in differentiating them, while distributing them to different processors can also be harmful due to the communication overhead when extracting shared information. In contrast, P3C uses correlation-based clustering, where alternatives in the same cluster have high correlations but may differ significantly in mean performance. We prove that clustering together highly correlated alternatives can accelerate the R&S procedure. This advantage is uncovered by establishing a theoretical underpinning of the interaction between mean and correlation: adding correlation can yield a “separation” effect, which probabilistically amplifies good alternatives while suppressing the bad ones. Another intuitive explanation is that clustering highly correlated alternatives together effectively cancels out stochastic fluctuations in the same direction. The stronger the correlation, the more pronounced this effect becomes. These concepts parallel the CRN technique, which introduces positive correlation artificially to expedite pairwise comparisons.

R&S problems can be formulated as either fixed-precision or fixed-budget paradigm (Hunter and Nelson 2017), and most of the prominent large-scale methods adopt the former formulation.

However, in certain large-scale applications such as NAS, achieving a high confidence level is often infeasible due to the limited availability of public datasets. Our screening-free version of P3C, referred to as P3C-GBA, uses a sequential generalized budget allocation (GBA) algorithm equipped with stopping rules, similar to Branke et al. (2007) and Eckman and Henderson (2022). P3C-GBA is applicable to both formulations, depending on the stopping rule employed. P3C is a flexible framework that also accommodates the use of fully-sequential procedures with screening, such as GSP (Ni et al. 2017) and KT, significantly outperforming their counterparts without using P3C.

A consensus in large-scale R&S literature is that there may exist a large number of acceptably *good* alternatives with means lying within a δ range around the best one (Ni et al. 2017, Pei et al. 2022). In such “low-confidence scenarios” (Peng et al. 2017) characterized by similar means and finite sample sizes, we find that correlation information becomes a crucial factor in evaluating alternatives. Relying solely on mean information would neglect alternatives with a much higher probability of being the best. Therefore, we select the alternative that maximizes the individual probability of correct selection (PCS), termed *probabilistic optimal selection* (P-OS), instead of simply choosing the largest sample mean. Similar probability-based selection policies are often adopted in the Bayesian framework (Peng et al. 2016, Russo 2020, Kim et al. 2022), and the integration of similarity information into selection policies is explored in Zhou et al. (2023). Additionally, we prove that P-OS can identify an alternative within each cluster that not only has a good mean performance but also effectively represents the cluster’s collective information. Specifically, a *representative* alternative refers to a “central” one which exhibits strong correlations with other alternatives within the same cluster. This viewpoint is the foundation of Principal Component Analysis (PCA), a successful dimension reduction method in machine learning (Al-Kandari and Jolliffe 2001, Shlens 2014). With P-OS, P3C is analogous to PCA-based variable selection techniques (Jolliffe 1972, Enki et al. 2013).

The main contributions of this paper can be summarized as follows.

- We propose P3C procedures for solving large-scale R&S problems. We establish a theoretical underpinning of the interaction between mean and correlation information and prove that correlation-based clustering can achieve rate-optimal sample complexity reduction.

- We introduce a new selection policy, named P-OS, tailored for large-scale scenarios, along with a corresponding GBA sampling policy.
- We propose a parallelizable few-shot alternative clustering algorithm, denoted as \mathcal{AC}^+ . This algorithm eliminates the need to estimate the entire correlation matrix and only requires a small submatrix, effectively addressing the challenges of large-scale clustering. We introduce the *probability of correct clustering* (PCC) to quantify the clustering quality.

2. Problem Formulation

Let $\mathcal{P} = \{1, 2, \dots, p\}$ denote the index set for all p alternatives. We adopt a Frequentist framework, and the output of alternative $i \in \mathcal{P}$ is a random variable X_i . We assume that the population distribution of the random vector (X_1, X_2, \dots, X_p) is multivariate normal $N(\boldsymbol{\mu}, \Sigma_{p \times p})$, where $\boldsymbol{\mu} = (\mu_1, \dots, \mu_p)$ is the mean vector and $\Sigma_{p \times p}$ is the covariance matrix. Let x_{ij} denote the j th simulation observation of alternative i . The observation vectors $(x_{1j}, x_{2j}, \dots, x_{pj}) \sim N(\boldsymbol{\mu}, \Sigma_{p \times p})$ are independently and identically distributed. We assume

$$\text{cov}(x_{im}, x_{jn}) = \begin{cases} 0 & m \neq n \\ \text{cov}(X_i, X_j) & m = n \end{cases},$$

where $\text{cov}(X, Y)$ represents the covariance between random variables X and Y . Let N_i denote the individual sample size allocated to alternative i and \bar{x}_i be the sample average, then $\text{cov}(\bar{x}_i, \bar{x}_j) = \frac{\text{cov}(X_i, X_j)}{\max(N_i, N_j)}$. The objective of R&S is to identify the true best alternative $[1] = \arg \max_{i \in \mathcal{P}} \mu_i$.

The correlation within the distribution arises from the influence of common latent factors, reflecting the similarity between alternatives. Suppose that the p alternatives come from k non-overlapping clusters: $\mathcal{G}_1, \dots, \mathcal{G}_k$ ($k \leq p$) with cardinality $|\mathcal{G}_j| = p_j$ ($\sum_{j=1}^k p_j = p$). G is a mapping from \mathcal{P} to $\{1, 2, \dots, k\}$, where $G(i) = j$ if alternative i belongs to \mathcal{G}_j . $\Pi = (G(1), G(2), \dots, G(p)) \in \mathbb{R}^p$ represents the true cluster partition of p alternatives (unknown) and we need sampling to recover it. Alternatives within the same cluster are highly correlated (although their mean performances may vary considerably), whereas alternatives from different clusters are less correlated. We assume that the Pearson correlation coefficient between any two alternatives belonging to the same cluster

exceeds that between any two alternatives from different clusters. Notably, the independent case is also included by setting $p = k$.

ASSUMPTION 1. $r_{ij} > r_{mn}$ for all $i, j, m, n \in \mathcal{P}$ such that $G(i) = G(j)$ and $G(m) \neq G(n)$, where r_{ij} denotes the correlation coefficient between X_i and X_j and $0 < r_{ij} < 1$.

3. The Framework of Parallel Correlation-Based Clustering and Conquer

Since the alternatives in the same cluster reflect common latent factors and attributes, one may select a *representative* alternative from each cluster to reduce complexity. For example, if the outputs of two alternatives satisfy $X_1 = X_2 + \epsilon$ where ϵ represents white noise, we only need to simulate one of them to gain knowledge about both alternatives. The development of P3C procedures is inspired by this intuition.

3.1. Clustering and Conquer

As outlined in Procedure 1 and Figure 2, P3C starts with an initialization Stage 0. Then, in Stage 1, we continue sampling and then cluster alternatives based on correlations. The sample size can be determined in advance based on the required clustering accuracy. Additionally, the novel few-shot clustering algorithm \mathcal{AC}^+ , detailed in Chapter 5, enables the effective parallelization of both Stage 0 and Stage 1 in large-scale problems. Upon completion of Stage 1, the alternatives of the same cluster are sent to a single processor. During Stage 2, we continue sampling and then select the local best within each cluster. This stage exclusively involves the comparison within the cluster, without any information exchange between clusters. The sampling strategy here is flexible, accommodating various existing fully-sequential methods like KT and GSP, which typically involve screening, i.e., discarding clearly inferior alternatives early on. We also provide a screening-free version that employs a sequential GBA sampling algorithm with stopping rules, referred to as P3C-GBA (see Chapter 6). In Stage 3, we simulate and compare these k selected local bests to determine the final winner. Regarding statistical validity, if each cluster achieves a precision of $1 - \alpha_1$ in Stage 2, and if Stage 3 achieves $1 - \alpha_2$, the overall statistical guarantee will be $1 - (\alpha_1 + \alpha_2)$. In practice, we set α_1 to be much larger than α_2 since p is much larger than k .

Procedure 1 Parallel Correlation-based Clustering and Conquer (P3C)

Stage 0 (Initialization). Simulate N_0 times for each alternative and estimate the correlation matrix.

Stage 1 (Alternative clustering). Continue sampling. Perform clustering algorithm \mathcal{AC}^+ to group all p alternatives into k correlated clusters. After that, assign the alternatives of the same cluster to one processor.

Stage 2 (Selecting the representative local best). Continue sampling (using KT, GSP or GBA) and calculate the P-OS within each cluster.

Stage 3 (Final comparison). R&S on the selected k local P-OSs and find the global optimal alternative.

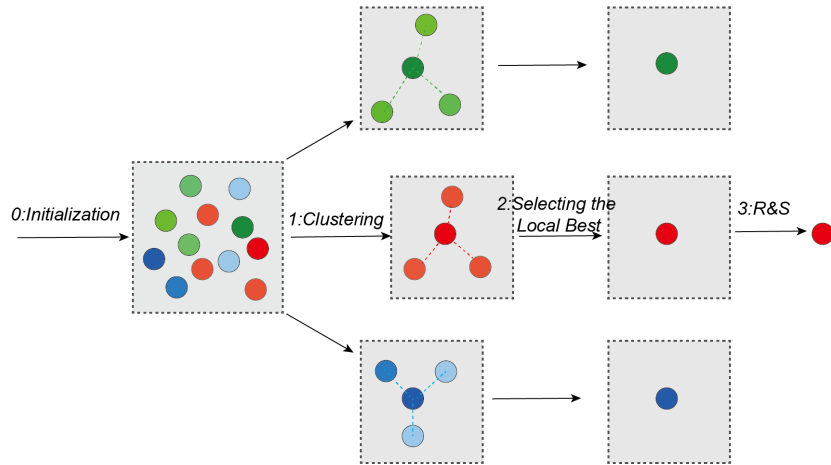


Figure 2 Parallel correlation-based clustering and conquer.

P3C can be viewed as a variant of the “divide and conquer” strategy (Ni et al. 2017, Zhong and Hong 2022). The first departure is that P3C performs correlation-based clustering and then systematically assigns alternatives from the same cluster to a single processor, rather than randomly assigning them. We prove that correlation-based clustering can bring rate-optimal sample complexity reduction. The second departure is the adoption of the aforementioned sequential GBA algorithm (optional). It can adapt to both fixed-precision and fixed-budget formulations. Moreover, it leverages correlation information and exhibits high sample efficiency in large-scale experiments.

3.2. Probabilistic Optimal Selection Policy

The third departure from the original “divide and conquer” is adopting a new selection policy. The selection policy τ is defined as a mapping from the information set to \mathcal{P} (Peng et al. 2016). In traditional R&S procedures, the selection policy is specified as $\tau^m = \arg \max_{i \in \mathcal{P}} \bar{x}_i$ (or maximizing the posterior mean in Bayesian framework), and correspondingly, the traditional PCS is defined as $\text{PCS}_{\text{trad}} \triangleq P(\bar{x}_{[1]} > \bar{x}_j, j \neq [1])$. To incorporate correlation information into the selection criterion, we borrow an idea from Bayesian R&S, which selects the one maximizing the posterior PCS rather than simply maximizing the posterior mean (Peng et al. 2016, Russo 2020, Kim et al. 2022). First, for any $\tau \in \mathcal{P}$, we define the individual PCS of τ as $\text{PCS}(\tau) \triangleq P(\bar{x}_\tau > \bar{x}_j, j \neq \tau)$. This is the natural generalization of traditional PCS as $\text{PCS}_{\text{trad}} = \text{PCS}([1])$. According to Hong et al. (2021), the statistical meaning of $\text{PCS}(\tau)$ is the probability of rejecting the null hypothesis that “ τ is *not* the true best”, serving as a metric to evaluate the performance of τ . Then the P-OS of \mathcal{P} is defined as the alternative maximizing $\text{PCS}(\tau)$:

$$\tau^* \triangleq \arg \max_{\tau \in \mathcal{P}} \text{PCS}(\tau). \quad (1)$$

This definition can be readily adapted to any cluster $\mathcal{G}_j \subseteq \mathcal{P}$, $j = 1, \dots, k$. In practice, $\text{PCS}(\tau)$ and τ^* are calculated by plugging in parameters estimated with samples collected so far. Naturally, the P-OS policy corresponds to a new statistical guarantee: $\text{PCS}(\tau^*)$, referred to as the *the most optimistic probability of correct selection* (moPCS). The moPCS can be used as a relaxed probability guarantee because $\text{moPCS} \geq \text{PCS}_{\text{trad}}$. In our large-scale AI experiments, moPCS can even be several tens of times higher than PCS_{trad} .

The benefits and properties of the P-OS policy, extensively discussed in Chapter 4, can be summarized as follows. First, the P-OS will converge to [1] as the sample size approaches infinity. Second, with *finite* samples, the P-OS policy is proved to select a desirable *representative* local best within each cluster that not only has a large mean but also exhibits high correlations with other cluster members. This brings us back to the intuition behind P3C, i.e., to reduce the problem

complexity by selecting a *representative* from each cluster. Third, while the analysis and methodologies in this paper remain valid for the traditional selection policy τ^m and performance metric PCS_{trad} (by letting $\tau^* = [1]$), the adoption of P-OS and moPCS is particularly advantageous in large-scale R&S problems with frequent occurrences of low-confidence scenarios. In such scenarios, correlation information plays a pivotal role in the probabilistic evaluation of alternatives. Relying solely on mean information would result in overlooking many alternatives that have a much higher probability of being the best (potentially even several times higher).

4. Theoretical Analysis of P3C: Understanding Mean-Correlation Interactions

In this chapter, a comprehensive theoretical analysis of P3C is presented. In Section 4.1, we delve into how mean and correlation information interact to influence individual PCS. This exploration not only clarifies the reasons why correlation-based clustering leads to improved sample efficiency, but also uncovers the properties of the P-OS policy. Unlike the well-studied mean-variance tradeoff, the mean-covariance interaction remains largely unexplored in existing literature. A related work by Peng et al. (2017) investigates the impact of “induced correlation”, which is induced by variance under the independent assumption, as opposed to actual correlation existing between alternatives. In Section 4.2, we quantify the sample complexity reduction brought about by correlation-based clustering and explore its influencing factors.

4.1. Interaction and Impact of Mean and Correlation on PCS

First, we introduce additional notations. We consider $\text{PCS}(\tau)$ and the P-OS of the entire set \mathcal{P} rather than a cluster within it, as the subsequent results can be naturally applied to any subset of \mathcal{P} . Let σ_i^2 denote the variance of X_i . For any alternative $\tau \in \mathcal{P}$, $\text{PCS}(\tau)$ can be rewritten as $P(y_1^\tau > -d_1^\tau, \dots, y_p^\tau > -d_p^\tau)$, where $y_i^\tau = \frac{\bar{x}_\tau - \bar{x}_i - (\mu_\tau - \mu_i)}{\sqrt{\lambda_i^\tau}}$, $d_i^\tau = \frac{\mu_\tau - \mu_i}{\sqrt{\lambda_i^\tau}}$, $\lambda_i^\tau = \text{var}(\bar{x}_\tau - \bar{x}_i) = \frac{\sigma_\tau^2}{N_\tau} + \frac{\sigma_i^2}{N_i} - 2 \frac{\text{cov}(X_\tau, X_i)}{\max(N_\tau, N_i)}$ and $i \in \mathcal{P} \setminus \{\tau\}$. The vector $\mathbf{y}^\tau = (y_1^\tau, \dots, y_{\tau-1}^\tau, y_{\tau+1}^\tau, \dots, y_p^\tau)$ follows distribution $N(0, \Phi^\tau)$, with the covariance matrix $\Phi^\tau = (\tilde{r}_{i,j}^\tau)_{(p-1) \times (p-1)}$ where $i, j \in \mathcal{P} \setminus \{\tau\}$. $\tilde{r}_{i,j}^\tau$ is the correlation coefficient between $\bar{x}_\tau - \bar{x}_i$ and $\bar{x}_\tau - \bar{x}_j$. Therefore, $|\tilde{r}_{i,j}^\tau| \leq 1$ is bounded. To simplify subsequent theoretical analysis, we assume that the range of $\tilde{r}_{i,j}^\tau$ is restricted to $\max\{-\sin(1) \approx -0.84, -|\frac{d_j^\tau}{d_i^\tau}|\} < \tilde{r}_{i,j}^\tau < \min\{1, |\frac{d_j^\tau}{d_i^\tau}|\}$. This assumption can be relaxed while still obtaining similar results.

4.1.1. Priority of Mean Information $\text{PCS}(\tau; \boldsymbol{\mu}, \Sigma, \{N_i\}_{i \in \mathcal{P}})$ is a function of mean, covariance and the allocation of sample sizes. Consistent with our intuition, $\text{PCS}(\tau)$ is monotonically increasing with respect to the mean μ_τ , and the P-OS τ^* will converge to the true best [1].

THEOREM 1. (1) $\text{PCS}(\tau)$ is differentiable with respect to $\boldsymbol{\mu} = (\mu_1, \dots, \mu_p)$ and $\frac{\partial \text{PCS}(\tau)}{\partial \mu_\tau} > 0$;
 (2) τ^* converges to [1] almost surely as $N_i \rightarrow \infty$ for $\forall i \in \mathcal{P}$.

Thus, $\text{PCS}(\tau)$ prioritizes mean information, favoring larger means under any correlation configuration. If an alternative's mean is distinctly prominent, it is highly likely to be selected as the P-OS. However, when the sample size is *finite* and numerous alternatives have similar means, known as the low-confidence scenario (Peng et al. 2017), correlation information may become the dominant factor. The following result demonstrates such a scenario.

PROPOSITION 1. Suppose that N_i is finite for all $i \in \mathcal{P}$ and there exists $\tau_0 \in \mathcal{P}$ such that $\tilde{r}_{i,j}^{\tau_0} > \tilde{r}_{i,j}^\tau$ for all $\tau \in \mathcal{P} \setminus \{\tau_0\}$ and all $i, j \in \mathcal{P}$, then there exists $\delta > 0$ such that if $|\mu_i - \mu_{\tau_0}| < \delta$ holds for all $i \in \mathcal{P} \setminus \{\tau_0\}$, we have $\tau^* = \tau_0$.

This proposition aligns with findings from Peng et al. (2016) within the Bayesian framework. $\tilde{r}_{i,j}^\tau$ is a function of correlations and is independent of mean parameters. Among those closely competing alternatives within a δ range, it is the correlation information that predominantly determines the P-OS, which may not necessarily be alternative [1].

4.1.2. The Derivative of PCS with respect to Correlation Information To further elaborate on the property of the P-OS policy and PCS, the following key result illustrates a more refined interaction effect between the mean and correlation.

THEOREM 2. Define $\mathcal{I}^+(\tau) \triangleq \{i \in \mathcal{P} \setminus \{\tau\} | \mu_i > \mu_\tau\}$ and $\mathcal{I}^-(\tau) \triangleq \{i \in \mathcal{P} \setminus \{\tau\} | \mu_i < \mu_\tau\}$, which are the index sets of the alternatives with larger and smaller mean than τ , respectively. Then $\forall i \in \mathcal{P} \setminus \{\tau\}$, $\frac{\partial \text{PCS}(\tau)}{\partial r_{\tau i}} = I_i + E_i$, where $I_i > 0$ for $i \in \mathcal{I}^-(\tau)$ and < 0 for $i \in \mathcal{I}^+(\tau)$.

REMARK 1. For simplicity, we drop the dependency of “ τ ” in I_i and E_i . The specific expressions of these terms can be found in the appendix. The analysis and methods presented in this paper do

not specify the computation of these terms but can help gain insights through the magnitude and sign of each term. The impact of variance information is also provided in the appendix.

As shown in Theorem 2, when considering $PCS(\tau)$ as a function of correlation coefficients $\{r_{\tau i}\}_{i \in \mathcal{P} \setminus \{\tau\}}$ while keeping other factors constant, the derivative $\frac{\partial PCS(\tau)}{\partial r_{i\tau}}$ is composed of two parts: the *mean-determined* (MD) term I_i and the *mean-independent* (MI) term E_i . The sign of the MD term depends on whether the mean μ_i is larger or smaller than μ_τ , whereas the sign of the MI term is independent of the mean. Temporarily setting aside the MI term, the correlations between τ and alternatives in $\mathcal{I}^-(\tau)$ impose a cumulative positive effect on $PCS(\tau)$, and conversely, correlations between τ and those alternatives in $\mathcal{I}^+(\tau)$ impose a cumulative negative effect. Consequently, the impact of correlation on $PCS(\tau)$ hinges on the order of mean μ_τ in $\{\mu_i\}_{i \in \mathcal{P}}$. If μ_τ is near the top, the number of alternatives in $\mathcal{I}^-(\tau)$ dominates, and then the cumulative positive effects surpass the cumulative negative effects. Therefore, increasing the correlations around τ is more likely to improve $PCS(\tau)$ (specifically, when $\tau = [1]$ and $\mathcal{I}^+(\tau) = \emptyset$, then increasing the correlation will certainly improve $PCS(\tau)$). On the contrary, if the alternative τ 's mean performance is poor, the influence of correlation is the opposite: increasing the correlation around τ will decrease $PCS(\tau)$.

Therefore, suppose that we are able to adjust the overall correlation level among the alternatives, a simple illustration of the effect is depicted in Figure 3. As shown in the regions I and IV, increasing the correlations can induce a “separation” effect, which may “amplify” good alternatives and “suppress” bad alternatives in terms of individual PCS, thus accelerating the R&S procedure. This phenomenon is analogous to the electrophoresis technique in chemistry, where an electric field propels particles with positive and negative charges in different directions to separate the mixture. Conversely, decreasing the overall correlation leads to an undesirable aggregation phenomenon (regions II and III). In practice, we cannot adjust the global correlation configuration within the distribution, but we can enhance the local correlation level on each processor using clustering techniques, thereby expediting the local R&S procedure. This is the rationale behind P3C's use of correlation-based clustering to enhance sample efficiency.

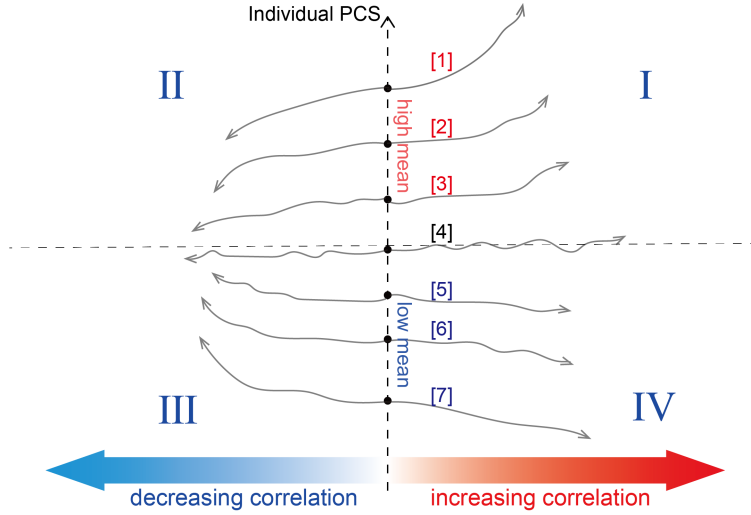


Figure 3 An illustrative example with 7 alternatives, where the top 3 alternatives [1], [2] and [3] exhibit high mean performances, and [5], [6] and [7] exhibit low mean performances.

4.1.3. The Orders of Magnitude of MD and MI Terms The analysis above overlooks the MI terms. Determining the signs of MI terms is challenging due to their complex dependencies on sample size and correlation structure. Therefore, to complete the analysis, it is necessary to establish the magnitudes of MD and MI terms to ascertain which term dominates. For a given vector \mathbf{d} and an index set S , we write \mathbf{d}_S the vector composed of the components from \mathbf{d} with indices S . Similar notations Σ_S are used for submatrices of matrix Σ . Let N denote the total sample size, i.e., $N = \sum_{i \in \mathcal{P}} N_i$.

ASSUMPTION 2 (Non-vanishing Individual Sample Size). $N_i \sim O(N_j)$, $\forall i, j \in \mathcal{P}$.

COROLLARY 1. *If Assumption 2 holds, $\forall i \in \mathcal{P} \setminus \{\tau\}$,*

(a) *There exists an index set $S \subseteq \mathcal{S}_{-i}^+(\tau) \triangleq \{j \in \mathcal{P} \setminus \{i, \tau\} \mid -\tilde{d}_j^\tau > 0\}$ such that*

$$|I_i| \sim \mathcal{O}\left(\sqrt{N} \cdot \exp\left(-\frac{\mathbf{d}_S^t (\Sigma_S^Z)^{-1} \mathbf{d}_S + (d_i^\tau)^2}{2}\right)\right), \quad (2)$$

$$|E_i| \sim \mathcal{O}\left(\exp\left(-\min_{j \neq i} \frac{(d_i^\tau)^2 + (d_j^\tau)^2}{2(1 + \arcsin(\tilde{r}_{i,j}^\tau))}\right)\right), \quad (3)$$

where $-\tilde{d}_j^\tau \triangleq -d_j^\tau + d_i^\tau \tilde{r}_{i,j}^\tau \sim \mathcal{O}(\sqrt{N})$ ($j \in \mathcal{P} \setminus \{\tau, i\}$), $\mathbf{d} = (-\tilde{d}_1^\tau, \dots, -\tilde{d}_p^\tau) \in \mathbb{R}^{p-2}$ and Σ^Z is a covariance matrix of p transformed variables which are given in the appendix;

(b) *When $\tau = [1]$, if $\tilde{r}_{i,j}^\tau < \epsilon_i \triangleq \min_{s \neq i} \sin\left(\frac{(d_s^\tau)^2}{(d_i^\tau)^2}\right)$ for any $j \neq i$, then $|E_i| \sim o(|I_i|)$.*

REMARK 2. Assumption 2 means that the sample size allocated to any alternative is of the same order (even though the proportion for some alternative may be extremely small) and can be sampled infinitely as N goes to infinity.

Since \tilde{d}_i^τ and d_i^τ are $\mathcal{O}(\sqrt{N})$, according to (a), both the MD and MI terms will decrease exponentially to 0 as the total sample size N increases. To facilitate comparison, we can rewrite the quadratic form in (2) and (3) by introducing $A_i > 0$ and $B_i > 0$, such that $|I_i| \sim \mathcal{O}(\sqrt{N}e^{-A_i N})$ and $|E_i| \sim \mathcal{O}(e^{-B_i N})$ for $i \in \mathcal{P} \setminus \{\tau\}$. Here, $A_i(\tau)$ and $B_i(\tau)$ are functions of τ and we drop it for simplicity. Whether the MD terms or MI terms dominate depends on the relative magnitudes of A_i and B_i . A key observation is: **when the mean of τ is high and ranks among the top alternatives, A_i tends to be lower than B_i , and thus the MD terms tend to be dominant.** This is because, as shown in Corollary 1(a), since $|\tilde{r}_{i,j}^\tau| < |\frac{d_j^\tau}{d_i^\tau}|$, the sign of $-\tilde{d}_j^\tau$ is equal to the sign of $-d_j^\tau$, which is determined by $(\mu_j - \mu_\tau)$. As the mean μ_τ increases, the number of indices j satisfying $-\tilde{d}_j^\tau > 0$ decreases, leading to a decrease in the cardinality of the subset S and subsequently reducing the quadratic term $\mathbf{d}'_S(\Sigma_S^Z)^{-1}\mathbf{d}_S$ in (2). This results in a smaller A_i , and the MD term is more likely to dominate. In particular, if $\tau = [1]$, the quadratic term $\mathbf{d}'_S(\Sigma_S^Z)^{-1}\mathbf{d}_S = 0$. Then, as shown in Corollary 1(b), the MD terms will certainly dominate over the MI terms under a boundedness condition on $\tilde{r}_{i,j}^\tau$. Therefore, based on the above observation, the following assumption is readily satisfied for the high-mean alternatives that are of interest to users.

ASSUMPTION 3 (**Sufficiently High Mean of τ**). $A_i(\tau) < B_i(\tau)$ for any $i \in \mathcal{P} \setminus \{\tau\}$.

4.1.4. Preference of P-OS policy Given the mean-correlation analysis above, we can also capture the types of alternatives that the P-OS policy is likely to select. For clarity, we roughly categorize all alternatives within a single cluster into four types based on their mean and correlation information (corresponding to the regions I, II, III, and IV in the Figure 3):

- Type I: high mean performance, high correlation;
- Type II: high mean performance, low correlation;
- Type III: low mean performance, low correlation;

- Type IV: low mean performance, high correlation.

The term “high (low) correlation” signifies a high (low) level of correlation between this alternative and others in the same cluster. We pick four alternatives $\tau_1, \tau_2, \tau_3, \tau_4$ from types I, II, III, and IV, respectively. While analyzing one of the four, we assume the absence of the other three in \mathcal{P} . According to Theorem 1, $PCS(\tau)$ prioritizes mean information and is monotonically increasing with respect to the mean. Thus, $PCS(\tau_1) > PCS(\tau_4)$ and $PCS(\tau_2) > PCS(\tau_3)$. We then compare τ_1 and τ_2 , both having high means. Therefore, we assume that both of them satisfy Assumption 3. We specify that τ_1 and τ_2 have identical mean and variance parameters. For each $i \in \mathcal{P} \setminus \{\tau_1, \tau_2\}$, we specify that $r_{\tau_1, i} = r_{\tau_2, i} + \Delta r_i$, where $\Delta r_i > 0$. With Theorem 2, Corollary 1 and Lagrange’s mean value theorem, we have the following corollary.

COROLLARY 2. *If Assumption 2 holds, and Assumption 3 holds for τ_1 and τ_2 ,*

$$PCS(\tau_1) - PCS(\tau_2) = \sum_{i \in \mathcal{I}^-} |I_i| \cdot \Delta r_i - \sum_{i \in \mathcal{I}^+} |I_i| \cdot \Delta r_i + o\left(\sum_{i \in \mathcal{I}^+ \cup \mathcal{I}^-} |I_i| \cdot \Delta r_i\right),$$

where each I_i is evaluated at a point $(r_{\tau_2, 1} + \xi \Delta r_i, \dots, r_{\tau_2, p} + \xi \Delta r_p) \in (-1, 1)^{p-1}$ and $\xi \in (0, 1)$. Since both τ_1 and τ_2 have high means, the set \mathcal{I}^- dominates over \mathcal{I}^+ , causing the first term on the right-hand side of the equation to be dominant. Consequently, $PCS(\tau_1) > PCS(\tau_2)$. In conclusion, alternative τ_1 maximizes the individual PCS and is selected as τ^* . Alternatives falling into Type I act as desirable *representatives* of this cluster, which not only have high mean performances but also effectively capture the information of the cluster. It’s worth noting that P-OS bears a profound underlying connection with PCA-based variable selection techniques (Jolliffe 1972) in machine learning (for a detailed comparison, see the appendix).

4.2. Rate-Optimal Sample Complexity Reduction

After understanding how correlation-based clustering leverages mean-correlation interaction to expedite the R&S process, we will now proceed with the specific calculation of the reduced sample complexity in fixed-precision R&S. In a parallel computing environment, we compare two distinct strategies for distributing alternatives across processors: (\mathcal{R}) randomly assigning an equal number

of alternatives to each processor, as in the original “divide and conquer” procedures; or (C) adopting a correlation-based clustering technique and assigning each cluster to a single processor.

We consider a scenario with k clusters ($k \ll p$), each containing $1 + \frac{p}{k}$ alternatives ($p + k$ in total), and k available parallel processors. The true clustering label is unknown, but we assume knowledge of the index of the local best in each cluster \mathcal{G}_j ($j = 1, \dots, k$), denoted as τ_j . To encompass all classic methods designed for the PCS_{trad} metric, we assume that τ_j has the largest mean within its cluster (Assumption 3 is readily satisfied) and thus $\text{moPCS} = \text{PCS}_{\text{trad}}$. Each local best is placed on a dedicated processor and will not be relocated thereafter. All k local bests share the same mean and variance. The means and variances of the remaining p alternatives are identical and are assigned to different processors using strategy \mathcal{R} or \mathcal{C} . Samples are simulated until each processor achieves $\text{PCS}_{\text{trad}} > 1 - \alpha$. The required total sample sizes in strategies \mathcal{R} and \mathcal{C} are denoted as N_R and N_C , respectively. Correlation coefficients within the same cluster are set to R , while those between different clusters are set to r , with a difference of $R - r = \Delta r$.

Due to the limitation of samples used for learning correlation information, the clustering accuracy in strategy \mathcal{C} may be < 1 . Given the randomness of simulation outputs, we introduce *probability of correct clustering* (PCC) to measure the statistical guarantee of clustering quality, defined as

$$\text{PCC} \triangleq P(\Pi_n = \Pi),$$

where $\Pi_n = (G_n(1), \dots, G_n(p)) \in \mathbb{R}^p$ is the partition result obtained by the employed clustering algorithm after processing n samples, with $G_n(i)$ being the cluster assignment of alternative i . Before proceeding to obtain the final results, the following lemma is needed in the proof as a supplement to Theorem 2.

LEMMA 1. $\forall i, j \in \mathcal{P} \setminus \{\tau\}$, $\frac{\partial \text{PCS}(\tau)}{\partial r_{ij}} \geq 0$. If Assumption 3 holds, then $\frac{\partial \text{PCS}(\tau)}{\partial r_{ij}} \sim o\left(\left|\frac{\partial \text{PCS}(\tau)}{\partial r_{i\tau}}\right|\right)$.

This lemma characterizes the impact of correlations $\{r_{ij}\}_{i,j \in \mathcal{P} \setminus \{\tau\}}$, which are *not* directly associated with τ , on $\text{PCS}(\tau)$. These correlations in the surrounding environment always have a non-negative impact, regardless of mean information. This further complements the argument that clustering

highly correlated alternatives can accelerate the R&S procedure. Additionally, under Assumption 3, the impact of $\{r_{ij}\}_{i,j \in \mathcal{P} \setminus \{\tau\}}$ is negligible compared to $\{r_{\tau i}\}_{i \in \mathcal{P} \setminus \{\tau\}}$, so it will not affect the aforementioned “separation” phenomenon induced by $\{r_{\tau i}\}_{i \in \mathcal{P} \setminus \{\tau\}}$. Finally, Theorem 3 quantifies the sample complexity reduction brought about by correlation-based clustering.

ASSUMPTION 4. *PCS(τ) is a monotonically increasing, differentiable and concave function with respect to the total sample size N .*

Assumption 4 means the use of a sensible sampling strategy, ensuring that PCS improves with an increase in total sample size. The concavity assumption means that as the sample size increases, the marginal improvement in PCS (upper bounded by 1) gradually diminishes.

THEOREM 3. *If Assumption 2 holds, and in the j -th processor ($j = 1, \dots, k$), Assumptions 3-4 hold for the local best τ_j , then there exist $\xi \in (0, 1)$ such that:*

$$\mathbb{E}(N_R - N_C) \geq \gamma \Delta r \left(PCC - \frac{1}{k} \right) p, \quad (4)$$

where

$$\gamma = \frac{\frac{\partial PCS^1}{\partial r_{i_0, \tau}}(\tau_1; \Sigma', N_0 + \xi(N_C - N_0))}{\frac{\partial PCS^1}{\partial N}(\tau_1; \Sigma, N_0 + \xi(N_C - N_0))},$$

with PCS^1 being the local PCS of the first processor, Σ and Σ' being two covariance matrices, $i_0 \in \mathcal{G}_1 \setminus \{\tau_1\}$ and N_0 being the initialization sample size.

REMARK 3. This result holds universally without the need for specifying the type of sampling procedure. The employed sampling procedure is reflected in the denominator of γ (i.e., $\frac{\partial PCS}{\partial N}$), influencing how fast PCS grows with the total sample size.

Correlation-based clustering ensures a positive reduction in sample complexity as long as $PCC > \frac{1}{k}$ (i.e., the clustering accuracy surpasses that of random clustering). Zhong and Hong (2022) emphasizes the importance of understanding the asymptotic behavior of the total sample size as p increases, with the theoretical lowest growth rate being $\mathcal{O}(p)$. Therefore, for any *efficient* sampling procedure that achieves the lowest sample size growth rate such as KT, an $\mathcal{O}(p)$ complexity reduction rate is the optimal without violating the theoretical limits. According to Theorem 3, P3C can

achieve this optimal reduction rate, given that the order of γ is at least $\mathcal{O}(1)$ for those *efficient* sampling procedures (refer to the appendix for the proof). Moreover, the amount of sample savings also depends on the gap Δr between intra-cluster correlation and inter-cluster correlation. If all alternatives are independent, i.e., $\Delta r = 0$, clustering would not yield any improvement.

5. Large-Scale Alternative Clustering

While PCC does not directly determine the final statistical validity of R&S, which only depends on the moPCS (or PCS_{trad}) of each cluster, a higher PCC, as shown in Theorem 3, can facilitate greater sample savings. Nevertheless, clustering in large-scale problems presents challenges, both computationally and statistically. To address these challenges and strive for a high PCC, inspired by a well-known few-shot learning approach in the deep learning literature, namely, Prototypical Networks (Snell et al. 2017), we propose a parallel alternative clustering algorithm \mathcal{AC}^+ . Following this, we detail the methodology for calculating the PCC.

5.1. Few-shot Alternative Clustering

In P3C, we cluster alternatives instead of observations, a concept known as variable clustering in statistical literature. A commonly used algorithm for this purpose is the hierarchical clustering algorithm (Jolliffe 1972), denoted as \mathcal{AC} . Suppose the number of clusters k is known. Initially, each alternative is treated as an individual group. In each iteration, the two groups with the maximum similarity R are merged until k groups remain. The choice of k is flexible. A practical choice is to set k equal to the number of available processors. The (empirical) similarity between two groups of alternatives, G^1 and G^2 , is quantified by $R(G^1, G^2) = \max_{i \in G^1, j \in G^2} \hat{r}_{ij}^n$, where \hat{r}_{ij}^n denotes the estimated r_{ij} using n samples. Since the conventional estimator, sample correlation \bar{r}_{ij}^n , may perform poorly for large p (Fan et al. 2020), an easily computable large-dimensional covariance estimator from (Ledoit and Wolf 2020) is provided in the appendix. Nonetheless, \mathcal{AC} requires estimating the entire $p \times p$ correlation matrix, and more importantly, cannot be parallelized.

The few-shot \mathcal{AC}^+ algorithm resolves the above issues (see pseudocode in the appendix). Initially, \mathcal{P} is split into two sets: the support set \mathcal{P}_s and the query set \mathcal{P}_q , with sizes p_s and p_q respectively,

where $k \leq p_s \ll p$. Next, alternatives in \mathcal{P}_s are grouped into k clusters using the \mathcal{AC} algorithm, efficiently handled on a single processor due to the moderate size of p_s . In each cluster \mathcal{G}_j ($j = 1, 2, \dots, k$), one *representative* alternative τ_j is chosen as the “prototype” of the cluster. Finally, each alternative in the query set \mathcal{P}_q is assigned to an existing cluster by identifying the most correlated prototype. This matching process can be parallelized by sending a copy of the k *prototypes* to each processor and then randomly assigning alternatives in \mathcal{P}_q to different processors. Given that $k \ll p$, the additional simulation cost for these copies is negligible. \mathcal{AC}^+ eliminates the need for estimating the entire correlation matrix and only requires a small submatrix.

As for the selection of the “prototype” within each cluster \mathcal{G}_j , the process is as follows. (i) Apply PCA to cluster \mathcal{G}_j to identify the first principal component $PC_{\mathcal{G}_j}$, which is a synthetic variable given by $PC_{\mathcal{G}_j} = \sum_{i \in \mathcal{G}_j} k_{ij} X_i$. Detailed calculations can be found in standard machine learning textbooks. In variable clustering literature, $PC_{\mathcal{G}_j}$ is often termed as the “latent component” of \mathcal{G}_j , proven to be the linear combination that maximizes the sum of squared correlations with the alternatives located in \mathcal{G}_j (Vigneau and Qannari 2003). The loading k_{ij} measures the correlation between the alternative i and $PC_{\mathcal{G}_j}$. (ii) Select the alternative with the largest loading k_{ij} as the *representative* “prototype” of \mathcal{G}_j (Al-Kandari and Jolliffe 2001):

$$\tau_j = \arg \max_{i \in \mathcal{G}_j} k_{ij}. \quad (5)$$

5.2. Computation of PCC

Next, we establish a computable lower bound for $\text{PCC}_{\mathcal{AC}^+}$, the statistical guarantee of \mathcal{AC}^+ . Let $\Gamma \triangleq \{(ab, ac) | G(a) = G(b), G(a) \neq G(c), a, b, c \in \mathcal{P}, a \neq b\}$ be the collection of pairs of overlapping intra-cluster and inter-cluster correlations. $\Gamma_s \triangleq \{(ab, ac) \in \Gamma | a, b, c \in \mathcal{P}_s\}$ and $\Gamma_q \triangleq \{(a\tau_i, a\tau_j) \in \Gamma | a \in \mathcal{P}_q, i = G(a), j \in \{1, 2, \dots, k\} \setminus \{i\}\}$ are two subsets of Γ . Fisher’s z transformation of correlation coefficients, defined as $z(r) \triangleq \frac{1}{2} \ln \frac{1+r}{1-r}$, is monotonically increasing in $(0, 1)$. Therefore, according to Assumption 1, $z(r_{ab}) > z(r_{ac})$ for any pair $(ab, ac) \in \Gamma$. Borrowing the idea of indifference zone in R&S literature, in the following proposition we strengthen Assumption 1 by introducing a correlation indifference parameter $\delta_c > 0$ and assume $z(r_{ab}) > z(r_{ac}) + \delta_c$.

PROPOSITION 2. *If Assumption 1 holds and all clusters have equal sizes, then*

$$PCC_{AC^+} \geq (1 - k(1 - 1/k)^{p_s}) P\left(\bigcap_{(ab,ac) \in \Gamma_s} \{\hat{r}_{ab}^n > \hat{r}_{ac}^n\}\right) P\left(\bigcap_{(ab,ac) \in \Gamma_q} \{\hat{r}_{ab}^n > \hat{r}_{ac}^n\}\right). \quad (6)$$

Let Γ_\star be either Γ_s or Γ_q . If $z(r_{ab}) > z(r_{ac}) + \delta_c$ for any $(ab, ac) \in \Gamma_\star$, then

$$P\left(\bigcap_{(ab,ac) \in \Gamma_\star} \{\hat{r}_{ab}^n > \hat{r}_{ac}^n\}\right) \geq \sum_{(ab,ac) \in \Gamma_\star} \Phi\left(\frac{\delta_c}{\sqrt{\frac{2(1-\bar{r}_{bc}^n)h(a,b,c)}{n-3}}}\right) - (|\Gamma_\star| - 1), \quad (7)$$

where $h(a, b, c) = \frac{1-f \cdot \bar{R}^2}{1-\bar{R}^2}$, with $\bar{R}^2(a, b, c) = \frac{(\bar{r}_{ab}^n)^2 + (\bar{r}_{bc}^n)^2}{2}$ and $f(a, b, c) = \frac{1-\bar{r}_{bc}^n}{2(1-\bar{R}^2)}$.

The computation of PCC_{AC^+} when cluster sizes are unequal, as well as the computation of PCC_{AC} can be found in the appendix. As $n \rightarrow \infty$, the lower bound of PCC_{AC^+} converges to $1 - k(1 - 1/k)^{p_s}$, approaching 1 in large-scale problems where p_s is in the hundreds or thousands, and k is significantly smaller than p_s . In practice, an excessively high PCC is not required (exceeding $1/k$ is sufficient). Moreover, with this computable lower bound, one can determine the required sample size to achieve a given clustering precision (see the appendix).

6. Generalized Budget Allocation under P-OS

For the P-OS policy and moPCS metric, we introduce a corresponding simulation resource allocation policy named GBA, which is sequential and is equipped with stopping rules. GBA is termed “generalized” because (i) it can accommodate both fixed-precision and fixed-budget constraints by employing different stopping rules: the former checks for a specified precision level, while the latter checks if the maximum budget is reached; (ii) it allows for correlation among alternatives; (iii) when $\tau^* = [1]$, it will reduce to an algorithm designed for the traditional PCS_{trad} metric.

6.1. Repeatedly Checking Stopping Rules

In this section, we elaborate on the GBA algorithm for the entire \mathcal{P} under fixed-precision constraints, which can be easily adapted to both specific clusters within \mathcal{P} and fixed-budget constraints. Branke et al. (2007) and Eckman and Henderson (2022) introduce the scheme of repeatedly checking stopping rules for various sampling policies, enabling early termination and sample savings.

GBA adheres to this approach (see Algorithm 1). In each iteration, a sample batch of size N_B is allocated according to a specialized policy. After the batch is simulated, the stopping rule is checked. The iterations continue until the stopping condition is first met. Regarding the calculation of stopping rules, we use the cheap Bonferroni lower bound (see inequality (8)). The other two commonly used calculation methods, the Slepian lower bound (Branke et al. 2007) and the equivalent one-dimensional integral (Peng et al. 2016), do not allow for correlation among alternatives. Please refer to Eckman and Henderson (2022) for more computational considerations.

Experiments show that the scheme of repeatedly checking stopping rules is notably sample-efficient in large-scale problems, even without explicit screening steps. This efficiency arises partly because, with a moderate batch size (e.g., 1-3 times the number of alternatives), the presence of numerous alternatives results in a sparse allocation: the majority receive zero samples in each iteration, once the allocation numbers are rounded to the nearest integer. Such sparsity in allocation can be viewed as implicit screening, eliminating the need for all pairwise comparisons. Additionally, the utilization of correlation information may also contribute to the high efficiency of GBA.

Algorithm 1 Generalized Budget Allocation (GBA)

Input: Batch size N_B , α , N_0 initialization samples

Step 0. Calculate P-OS τ^* and estimate the covariance using the initialization samples.

Step 1 (Batch allocation policy). If τ^* has the maximum mean (i.e., Case (a)), calculate the optimal sample allocation $\{N_i^*\}_{i \in \mathcal{P}}$ with (EC.31). Otherwise (i.e., Case (b)), set $N_j^* = 0$ for any $j \in \mathcal{I}^+(\tau^*)$ and calculate $\{N_i^*\}_{i \in \mathcal{P} \setminus \mathcal{I}^+(\tau^*)}$ with (EC.31) by replacing $\Omega = \mathcal{P} \setminus \{\tau^*\}$ with $\mathcal{I}^-(\tau^*)$.

Step 2. Perform additional N_i^* simulations for the alternative $i = 1, 2, \dots, p$.

Step 3 (Checking stopping rules). Update estimators of means, covariance matrix and τ^* . Check whether it is Case (a) or Case (b). Calculate moPCS with (8). If $\text{moPCS} > 1 - \alpha$, stop; otherwise, go to Step 1.

6.2. Allocation Policy

Next, we design the allocation policy for each batch (see Step 1 of Algorithm 1). Suppose the batch size is fixed at N_B , the optimal allocation $\{N_i^*\}_{i \in \mathcal{P}}$ maximizes moPCS under a fixed budget constraint. Given τ^* , we adopt the Bonferroni lower bound of moPCS as the surrogate objective:

$$\text{moPCS} \geq \sum_{i \in \mathcal{P} \setminus \{\tau^*\}} \Phi(d_i^{\tau^*}) - (p-2) \geq (p-1) \min_{i \in \mathcal{P} \setminus \{\tau^*\}} \Phi(d_i^{\tau^*}) - (p-2). \quad (8)$$

Therefore, $\{N_i^*\}_{i \in \mathcal{P}}$ is equivalent to the solution to

$$\max_{\sum_{i=1}^p N_i = N_B} \min_{j \in \mathcal{P} \setminus \{\tau^*\}} \Phi(d_j^{\tau^*}). \quad (9)$$

Case (a): If $\tau^* = [1]$, then $\mathcal{I}^+(\tau^*) = \emptyset$ and $\text{moPCS} = \text{PCS}_{\text{trad}}$. The optimization problem (9) is equivalent to the correlated budget allocation (CBA) in Fu et al. (2007). The solution $\{N_i^*\}_{i \in \mathcal{P}}$ can be found in the appendix (EC.31).

Case (b): If $\tau^* \neq [1]$, then $\mathcal{I}^+(\tau^*) \neq \emptyset$. As suggested by Proposition 1, this situation often occurs in low-confidence scenarios with small mean differences and finite sample sizes. \mathcal{P} consists of three parts: $\mathcal{I}^+(\tau^*)$, $\mathcal{I}^-(\tau^*)$, and τ^* itself. In GBA, mean and correlation are estimated using observations collected so far, and then the individual PCS and τ^* are updated in each iteration. We then check whether τ^* is equal to $[1]$ (Case (a) or Case (b)). According to Theorem 1, as iterations progress and the total sample size N tends to infinity, $\tau^*(N)$ converges to $[1]$. Simultaneously, the set $\mathcal{I}^+(\tau^*(N))$ gradually diminishes. Assuming the monotonicity of this diminution, a non-trivial fact is that allocating a larger sample size to $\mathcal{I}^+(\tau^*)$ will unexpectedly reduce moPCS.

ASSUMPTION 5. *The cardinality $|\mathcal{I}^+(\tau^*(N))|$ is non-increasing with respect to N .*

PROPOSITION 3 (Negative Effect of Sample Size). *Suppose Assumption 2 and Assumption 3 hold for τ . For $i \in \mathcal{P} \setminus \{\tau\}$, the derivative of $\text{PCS}(\tau)$ with respect to N_i is given by $\frac{\partial \text{PCS}(\tau)}{\partial N_i} = I'_i + o(I'_i)$. If $N_\tau \geq N_i$ or $r_{\tau i} < \frac{\sigma_i}{2\sigma_\tau}$, then $I'_i < 0$ for $i \in \mathcal{I}^+(\tau)$ and $I'_i > 0$ for $i \in \mathcal{I}^-(\tau)$. Assuming Assumption 5 holds, the condition “ $N_{\tau^*} \geq N_i$ ” is consistently satisfied for $i \in \mathcal{I}^+(\tau^*)$ throughout the execution of Algorithm 1.*

Therefore, GBA allocates zero samples to alternatives within $\mathcal{I}^+(\tau^*)$ in each iteration. Then, among the remaining alternatives in $\mathcal{P} \setminus \mathcal{I}^+(\tau^*)$, τ^* has the largest mean. Therefore, this transforms into Case (a), and we compute the optimal allocation $\{N_i^*\}_{i \in \mathcal{P} \setminus \mathcal{I}^+(\tau^*)}$ by replacing the entire \mathcal{P} with $\mathcal{P} \setminus \mathcal{I}^+(\tau^*)$. In practice, to ensure the validity of Assumption 2, we slightly modify the original GBA and transform it into an ϵ -greedy version: we allocate a small sample size ϵN to the alternatives in $\mathcal{I}^+(\tau^*)$, where $\epsilon > 0$ is sufficiently small. Any other sampling strategy can be adjusted similarly to satisfy Assumption 2. The proposed allocation policy in the Step 1 of Algorithm 1 is equivalent to CBA in high-confidence scenarios (i.e., Case (a)) but it has significant advantages in low-confidence scenarios (i.e., Case (b)). These low-confidence situations are commonly encountered in large-scale R&S problems, particularly in the context of complex AI problems like NAS, due to the limited availability of public datasets and the intricate stochastic nature of neural networks.

7. Numerical Experiments

In Section 7.1, we provide a simple example to illustrate some key theoretical results of this paper, including the mean-correlation interaction (Theorem 2 and Lemma 1) and the negative effect of sample size (Proposition 3), which are the foundations of P3C and GBA, respectively. In Section 7.2, we test the performance of P3C under fixed-precision constraints and the PCS_{trad} metric. In Section 7.3, we test the performance of P3C under fixed-budget constraints, emphasizing the advantages of using the P-OS policy, moPCS metric, and GBA sampling policy.

7.1. Illustrative Example

Consider a group of 5 alternatives: $(X_1, X_2, X_3, X_4, X_5)$, each following a normal distribution. The mean and covariance parameters are given by $\boldsymbol{\mu} = (\mu_1, \mu_2, \mu_3, \mu_4, \mu_5) = (2.1, 2.0, 1.95, 1.9, 1.9)$ and

$$\Sigma = \begin{pmatrix} 0.1 & x & x & x & x \\ x & 0.1 & 0.01 & 0.01 & y \\ x & 0.01 & 0.1 & 0.01 & y \\ x & 0.01 & 0.01 & 0.1 & y \\ x & y & y & y & 0.1 \end{pmatrix}.$$

All alternatives share the same variance. Alternative 1 has the largest mean, and its covariance with other alternatives is x ($0 \leq x < 0.1$). Alternative 5 is the poorest performer, and its covariance with alternatives 2, 3 and 4 is y ($0 \leq y < 0.1$). To illustrate the proposed mean-correlation interaction theory (Theorem 2, Figure 3 and Lemma 1), we calculate PCS(1) and PCS(5) with different x and y , keeping the mean and variance parameters constant. The sample size for each alternative is 10 (total sample size $N = 50$). Table 1 presents the values of PCS(1) and PCS(5) when x takes on the values of 0.01, 0.02, 0.03, and 0.05, and y takes on the values of 0, 0.02, 0.04, and 0.06, respectively (there is no value in the table for $x = 0.05$ and $y = 0.06$ because Σ is not positive definite). This experiment is of a small scale, and the actual values of individual PCS are calculated using Monte Carlo numerical integration. The experimental results align with our theory of mean-correlation interaction: increasing correlation promotes alternatives with large means while suppressing those with small means. When y is held constant, PCS(1) increases as x increases, consistent with Theorem 2. When x is fixed, PCS(1) also increases with the growth of y , where y represents correlations between alternative 5 and alternatives 2-4, not directly associated with alternative 1. This result is consistent with Lemma 1. On the contrary, PCS(5) decreases as x (or y) increases.

Table 1 PCS(1) and PCS(5) with Different x and y ($N = 50$).

	$y = 0$		$y = 0.02$		$y = 0.04$		$y = 0.06$	
	PCS(1)	PCS(5)	PCS(1)	PCS(5)	PCS(1)	PCS(5)	PCS(1)	PCS(5)
$x = 0.01$	0.6707	0.0349	0.6741	0.0269	0.6875	0.1777	0.6879	0.0051
$x = 0.02$	0.6852	0.0331	0.6904	0.0255	0.7003	0.0168	0.7018	0.0050
$x = 0.03$	0.6979	0.0288	0.7141	0.0233	0.7171	0.0154	0.7274	0.0048
$x = 0.05$	0.7506	0.0197	0.7662	0.0166	0.7690	0.0119	\	

Next, we illustrate the negative effect of sample size on moPCS in low-confidence scenarios. We set $x = 0.05$, $y = 0.01$, and the sample sizes for alternatives 1-5 are $N_1, 10, 5, 5,$ and 5 respectively. The aforementioned mean parameter configuration μ represents a high-confidence scenario, where the mean of alternative 1 is noticeably higher than that of the other alternatives. Therefore, as

shown in the “high confidence scenario” row of Table 2, alternative 1 maximizes individual PCS and is selected as the P-OS. Below, to construct a low-confidence scenario, we reduce the mean of alternative 1 and modify the parameter configuration to $\boldsymbol{\mu}' = (2.01, 2.0, 1.95, 1.9, 1.9)$. In this low-confidence scenario, the correlation parameter becomes the dominant factor. Alternative 2 maximizes individual PCS and is selected as the P-OS. Alternative 1 has a larger mean than the P-OS and thus belongs to the set $\mathcal{I}^+(\tau^*)$. The individual PCS, moPCS, PCS_{trad} and P-OS for N_1 values of 5, 6, 7, 8, 9, and 10 are presented in Table 2. Consistent with Proposition 3, increasing the sample sizes of alternatives in $\mathcal{I}^+(\tau^*)$ leads to a decrease in moPCS. The presence of this negative effect is precisely why GBA’s allocation policy surpasses CBA in large-scale problems. The comparison of GBA’s and CBA’s experimental performance is discussed in Section 7.3.

Table 2 P-OS and Various Metrics in Different Scenarios and with Different N_1 .

Scenario		PCS(1)	PCS(2)	PCS(5)	PCS_{trad}	moPCS	P-OS
High confidence scenario	$N_1 = 5$	0.6010	0.1913	0.0512	0.6010	0.6010	alt. 1
Low confidence scenario	$N_1 = 5$	0.2900	0.3168	0.1042	0.2900	0.3168	alt. 2
	$N_1 = 6$	0.2762	0.3113	0.1074	0.2762	0.3113	
	$N_1 = 7$	0.2672	0.3068	0.1122	0.2672	0.3068	
	$N_1 = 8$	0.2580	0.3036	0.1179	0.2580	0.3036	
	$N_1 = 9$	0.2516	0.3005	0.1205	0.2516	0.3005	
	$N_1 = 10$	0.2461	0.2976	0.1198	0.2461	0.2976	

7.2. Fixed-precision R&S: Drug Discovery

In this section, we test the performance of P3C in the context of the narcotic analgesics drug discovery problem introduced in Negoescu et al. (2011). It studies a set of 6,7-Benzomorphans, which have 5 sites where substituents can be attached (see Figure 4(a)). Specifically, there are 11, 8, 5, 6, and 11 possible substituents for sites 1 to 5, respectively. Additionally, each compound can be positively, negatively, or neutrally charged. Consequently, there are $11 \times 8 \times 5 \times 6 \times 11 \times 3 =$

8.712×10^4 available alternative drugs in this large-scale R&S problem. As illustrated in Figure 4(b), a clear pattern of correlation-based clustering emerges in an example comprising 128 drugs. Simulation data are generated based on the Free-Wilson model: *the value of the drug = value of the base molecule + value of atom at site 1 + \dots + value of atom at site 5*, where the value of each atom is assumed to be an independent normal random variable (latent factor). The mean parameter of each atom is estimated through regression on experimental data from Katz et al. (1977), and the variance is randomly generated from a normal distribution $N(0, 0.1)$ (excluding negative values). We adopt the fixed-precision formulation of R&S. Our objective is to identify the best drug and ensure a precision of $1 - \alpha = 0.9$. The precisions for stage 2 and stage 3 are $1 - \alpha_1$ and $1 - \alpha_2$, respectively ($\alpha_1 + \alpha_2 = 0.1$). We set $\alpha_1 = 0.09$ and $\alpha_2 = 0.01$.

The P3C is compared with the traditional stage-wise procedure in Rinott (1978), the Good Selection Procedure (GSP) in Ni et al. (2017) and the Knockout Tournament (KT) procedure in Zhong and Hong (2022). However, these benchmarks are based on PCS_{trad} and do not accommodate the newly proposed P-OS policy and moPCS metric. Therefore, in this subsection, we focus on evaluating P3C's performance under the classical PCS_{trad} metric. The screening method used in KT relies on the indifference zone assumption, whereas GSP's screening method does not. To ensure a fair comparison, we replace the screening method in GSP with one based on the indifference zone assumption from Jeff Hong (2006). We also modify P3C slightly to incorporate the indifference zone assumption. According to the Lemma 3 in Zhong and Hong (2022), each alternative has a maximum sample size under indifference-zone assumption. If the maximum sample size is reached, the sampling process stops (though experimental results suggest this rarely occurs). We set the initialization sample size as $N_0 = 20$ and the indifference zone parameter as $\delta = 0.1$. The correlation estimation and clustering in P3C are exclusively based on the initialization samples.

P3C is a flexible framework that can accommodate various sampling procedures. To separately demonstrate the improvements brought by (i) correlation-based clustering and (ii) the GBA sampling policy, we provide three versions of P3C: P3C-GBA, P3C-EA, and P3C-KT. P3C-GBA

employs both (i) and (ii). P3C-EA employs (i) but uses equal allocation (EA) sampling policy within each cluster. It also adopts the scheme of repeatedly checking the stopping rules. By comparing P3C-GBA and P3C-EA, we can demonstrate the improvements brought about by (ii). P3C-KT employs (i) and uses KT for selecting local best within each cluster. By comparing KT and P3C-KT, we can demonstrate the improvements brought about by (i).

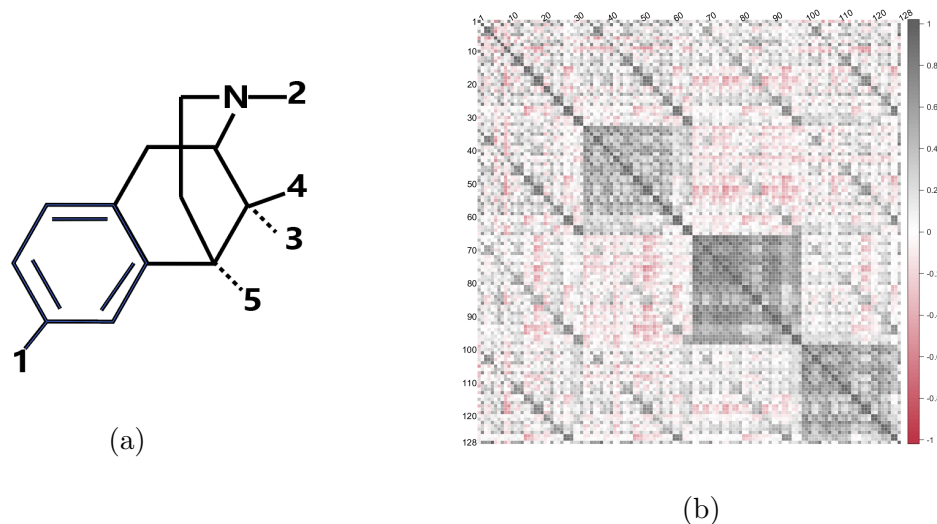


Figure 4 (a) 5 substituent locations. (b) Clustering phenomenon in drug correlations. Black points represent highly correlated drugs.

We conduct experiments on a commercial cloud platform and set up a computing cluster with 104 processors. Accordingly, k is set to 104. The experiments are conducted under the parallel computing environment of the MATLAB Parallel Computing Toolbox. The experiments are repeated 20 times, and averages are taken. Table 3 and Figure 5 present the required sample sizes for P3C-GBA, P3C-EA, P3C-KT, Rinott, GSP, and KT methods across different p . The classical stage-wise Rinott method requires an enormous amount of computational resources, necessitating 30-50 times the sample size of fully-sequential benchmarks such as KT and GSP. Therefore, screening has long been considered as the key to improving sample efficiency. Surprisingly, even without any screening, in Figure 5 we can see that P3C-GBA significantly outperforms KT and GSP. When $p = 2^{15}$, P3C-GBA only requires 60% of the sample size needed by KT and GSP. Comparing P3C-EA with

P3C-GBA shows that the GBA sampling policy results in an average 38% improvement. Comparing KT with P3C-KT, correlation-based clustering contributes to an average reduction in sample complexity of 47%. It can be observed from Figure 5 that the slope of the line representing KT decreases after applying P3C. This indicates a reduction in sample complexity of $O(p)$, consistent with Theorem 3.

In the comparison, P3C-KT and P3C-GBA are the top two performers, with P3C-GBA outperforming P3C-KT in large-scale scenarios. During each GBA iteration, the total sample size N_B for each processor is set to twice the number of alternatives on that processor. After rounding the allocation number to the nearest integer, over 90% of alternatives receive no samples during each iteration. This implicit screening significantly enhances sample efficiency. Additionally, GBA's utilization of correlation information may also contribute to its high efficiency.

Table 3 The Required Sample Size ($\times 10^4$) with Different Number of Alternatives

p	2^7	2^9	2^{11}	2^{13}	2^{14}	2^{15}	2^{16}
Rinott	2.23	9.26	156.27	945.02	2718.36	6268.69	15519.91
P3C-GBA	0.42	1.64	8.72	29.36	49.79	129.50	254.13
P3C-EA	0.70	2.69	10.86	50.39	71.40	196.60	433.08
P3C-KT	0.48	1.99	8.04	32.57	59.05	117.05	298.14
KT	0.73	3.77	13.04	57.44	97.00	222.12	385.57
GSP	0.96	4.88	15.50	37.29	81.87	210.31	472.67

According to Theorem 3, PCC significantly influences the performance of P3C. Employing the \mathcal{AC}^+ algorithm, we investigate $\text{PCC}_{\mathcal{AC}^+}$ under different sample sizes and different sizes of the support set ($p_s = 25, 50, 75, 100, 150$). We focus on the first 1024 drugs, set the cluster number to $k = 8$, and assume equal sizes for each cluster. The result is shown in Figure 6. As the sample size approaches infinity, consistent with Proposition 2, $\text{PCC}_{\mathcal{AC}^+}$ converges to $1 - k(1 - 1/k)^{p_s}$

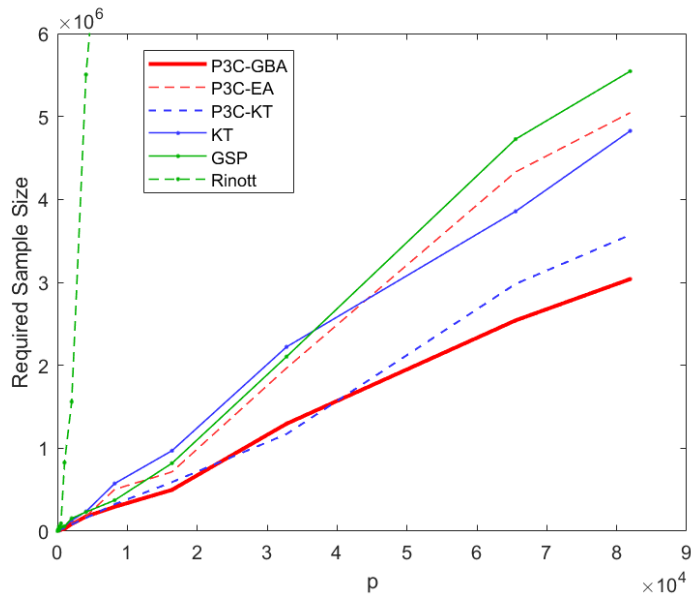


Figure 5 The required total sample size with different number of alternatives p .

(denoted as $P(D)$), which is less than 1. Larger p_s values lead to a larger $P(D)$. At $p_s = 25$, the PCC is notably constrained by the $P(D)$ term and cannot exceed 0.3. As p_s increases to 50, PCC approaches acceptably close to 1. Although the maximum PCC value of \mathcal{AC}^+ with $p_s = 50$ is lower compared to that of larger p_s , the growth rate of \mathcal{AC}^+ with $p_s = 50$ is the fastest till convergence. This could be attributed to the less efficient \mathcal{AC} algorithm used for clustering in the support set. As the size of the support set p_s increases, it significantly hampers overall PCC.

7.3. Fixed-budget R&S: Neural Architecture Search

The general NAS problem can be divided into two phases: architecture search (including search space and search strategy) and architecture performance estimation. However, training and evaluating neural networks can often be resource-intensive. Suppose that we have already obtained a set \mathcal{P} of p alternative architectures through certain search methods, the best architecture is defined as the one that maximizes generalization accuracy:

$$[1] \triangleq \arg \max_{i \in \mathcal{P}} \mathbb{E}(\text{ACC}_i), \quad (10)$$

where ACC_i is the accuracy of alternative i and the expectation is computed over the probability space of all of the unseen data points. It is impossible to calculate the expectation in (10) exactly,

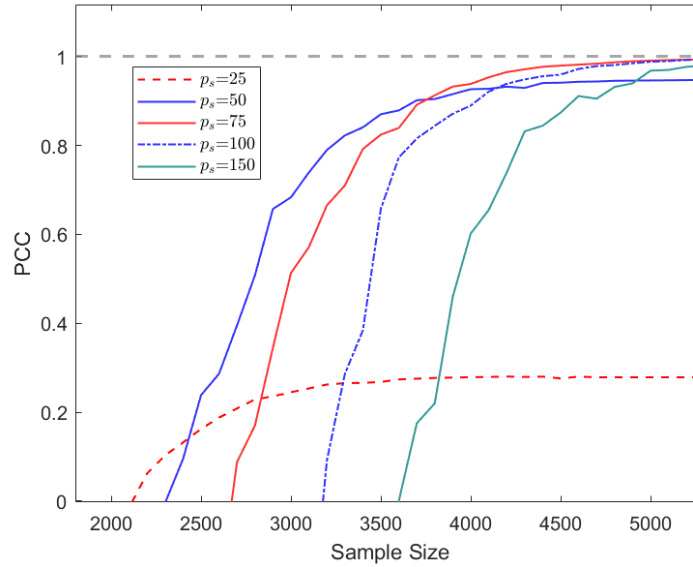


Figure 6 Comparison of PCC_{AC+} with different support set sizes p_s .

so we estimate it using Monte Carlo over the test dataset. Therefore, NAS can be viewed as a discrete simulation optimization problem, where the simulation model is a neural network. Testing one architecture on a batch of test data corresponds to one simulation run, and the accuracy is the simulation output. Given the limited size of the test dataset, which corresponds to a finite amount of simulation resources, we formulate NAS as a fixed-budget R&S problem. In this experiment, P3C is compared against EA, CBA in Fu et al. (2007) and FBKT in Hong et al. (2022). Additionally, FBKT, CBA and EA are also implemented in a parallel computing environment using “divide and conquer” strategy: in Stage 1, alternatives are randomly allocated to different processors. In Stage 2, a local best is selected from each processor, and then in Stage 3, these selected local best alternatives are compared to determine the ultimate best.

Performance metric and selection policy. We conduct experiments under two metrics, i.e., moPCS and PCS_{trad} . The former adopts the P-OS policy. The latter adopts the τ^m selection policy.

Dataset. This experiment is performed on the *CIFAR-10* dataset, which is used for image classification tasks. The dataset is divided into two parts: 10000 images for the test set and the remaining 50000 images for the training set.

Search Phase. The search phase is implemented in PyTorch using the *Single-Path One-Shot* (SPOS) method (Guo et al. 2020), a state-of-the-art NAS algorithm. The search space is a single-path supernet composed of 20 choice blocks connected in series, each with 4 choices. Thus, the search space size is 4^{20} . In Zhong and Hong (2022), the problem dimension reaches 10^6 , but the architecture search phase at this scale is estimated to take over 500 hours in a virtual machine with a RTX 3090 (24GB) GPU. Therefore, in our experiment, we set the number of alternative architectures to be $p = 10^5$ (the extensive time consumption is attributed to the search algorithm, not P3C itself).

Ranking and selection. The R&S phase is conducted under the same parallel computing environment as described in Section 7.2. After obtaining 10^5 alternative architectures, we use P3C-GBA, P3C-CBA, CBA, FBKT and EA to allocate computational resources for performance evaluation and select the best one. In GBA, we perform only one iteration and allocate the total budget at once. One simulation observation corresponds to testing an architecture on a batch of 32 images. Therefore, the maximum sample size for each alternative is $\frac{10000}{32} \approx 312$. This experiment does not involve intentional use of CRN, and the initialization sample size $N_0 = 20$. The moPCS (or PCS_{trad}) values are directly estimated based on 1000 independent macro replications. The true best [1] (invisible to the users and used solely for the final PCS_{trad} calculation) is estimated by selecting the alternative with the highest accuracy on the entire test set. Moreover, in Stage 2, the moPCS (or PCS_{trad}) values vary across different processors. The overall moPCS (or PCS_{trad}) for Stage 2 is approximated by a weighted average based on the number of alternatives on each processor.

The experimental results under moPCS metric and P-OS policy are depicted in Figure 7(a), and the results under PCS_{trad} metric and τ^m selection policy are depicted in Figure 7(b). This experiment is a low-confidence scenario, where 95% of the alternatives' mean performances fall within the interval (0.878, 0.889). When comparing Figures 7(a) and (b), with identical sampling policies and budgets, moPCS is found to be significantly larger than PCS_{trad} , sometimes even by several tens of times. This indicates that in low-confidence scenarios, the maximum mean and the

maximum individual PCS are often inconsistent, identified as Case (b) in Section 6.2. Employing the P-OS policy along with the moPCS metric is advantageous in such a case. Otherwise, relying solely on mean information, the traditional selection policy and metric would overlook many alternatives that have a much higher probability of being the best.

As shown in Figure 7(a), P3C-GBA demonstrates the best performance under moPCS metric. The average moPCS of P3C-CBA is 0.13 larger than CBA, buttressing the improvement brought by P3C. The average moPCS of P3C-GBA is 0.10 larger than P3C-CBA. This demonstrates that in low-confidence scenarios characterized by frequent occurrence of Case (b), GBA significantly outperforms CBA. When using FBKT or EA, moPCS decreases with an increase in the total sample size, which may be attributed to the negative effect of sample size described in Proposition 3. Under PCS_{trad} metric, GBA is equivalent to CBA. The favorable theoretical properties of P3C still hold under this metric (by letting $\tau^* = [1]$). As shown in Figure 7(b), P3C-CBA/GBA significantly outperforms CBA and FBKT. Moreover, the rate of increase in PCS_{trad} with the growth of the total sample size is the highest when using P3C-CBA/GBA.

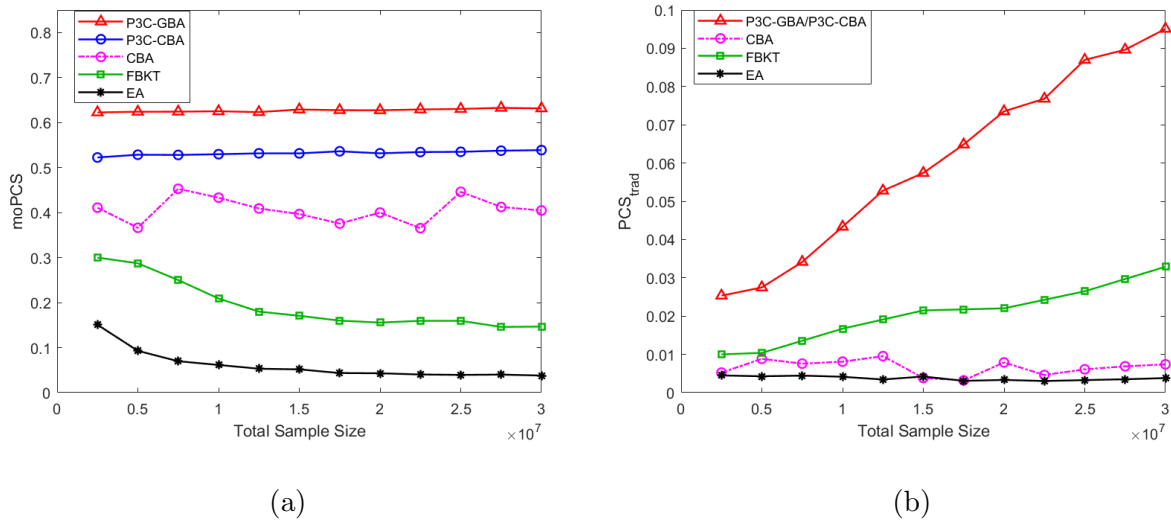


Figure 7 (a) Comparison of different R&S procedures under moPCS metric (b) Comparison of different R&S procedures under PCS_{trad} metric.

8. Concluding Remarks

This paper presents a user-friendly parallel computing framework for large-scale R&S problem, allowing for the easy integration of any existing R&S method. The “clustering and conquer” strategy, leveraging correlation information, overcomes the bottleneck of R&S methods under the independence assumption and achieves a rate-optimal sample complexity reduction. It can achieve improvements without the necessity of excessively high clustering accuracy. Additionally, experimental results demonstrate that a screening-free sampling strategy is highly sample efficient in large-scale scenarios due to the sparse allocation. As a future research direction, one may consider providing a detailed theoretical analysis for this sparsity phenomenon.

9. Acknowledgements

This work was supported in part by the National Natural Science Foundation of China (NSFC) under Grants 72325007, 72250065 and 72022001.

References

- Al-Kandari NM, Jolliffe IT (2001) Variable selection and interpretation of covariance principal components. *Communications in Statistics-Simulation and Computation* 30(2):339–354.
- Branke J, Chick SE, Schmidt C (2007) Selecting a selection procedure. *Management Science* 53(12):1916–1932.
- Eckman DJ, Henderson SG (2022) Posterior-based stopping rules for bayesian ranking-and-selection procedures. *INFORMS Journal on Computing* 34(3):1711–1728.
- Enki DG, Trendafilov NT, Jolliffe IT (2013) A clustering approach to interpretable principal components. *Journal of Applied Statistics* 40(3):583–599.
- Fan J, Li R, Zhang CH, Zou H (2020) *Statistical foundations of data science* (CRC press).
- Free SM, Wilson JW (1964) A mathematical contribution to structure-activity studies. *Journal of medicinal chemistry* 7(4):395–399.
- Fu MC, Hu JQ, Chen CH, Xiong X (2007) Simulation allocation for determining the best design in the presence of correlated sampling. *INFORMS Journal on Computing* 19(1):101–111.

- Guo Z, Zhang X, Mu H, Heng W, Liu Z, Wei Y, Sun J (2020) Single path one-shot neural architecture search with uniform sampling. *Computer Vision–ECCV 2020: 16th European Conference, Glasgow, UK, August 23–28, 2020, Proceedings, Part XVI 16*, 544–560 (Springer).
- Hong LJ, Fan W, Luo J (2021) Review on ranking and selection: A new perspective. *Frontiers of Engineering Management* 8(3):321–343.
- Hong LJ, Jiang G, Zhong Y (2022) Solving large-scale fixed-budget ranking and selection problems. *INFORMS Journal on Computing* 34(6):2930–2949.
- Hunter SR, Nelson BL (2017) Parallel ranking and selection. *Advances in Modeling and Simulation: Seminal Research from 50 Years of Winter Simulation Conferences*, 249–275 (Springer).
- Jeff Hong L (2006) Fully sequential indifference-zone selection procedures with variance-dependent sampling. *Naval Research Logistics (NRL)* 53(5):464–476.
- Jolliffe IT (1972) Discarding variables in a principal component analysis. i: Artificial data. *Journal of the Royal Statistical Society Series C: Applied Statistics* 21(2):160–173.
- Katz R, Osborne SF, Ionescu F (1977) Application of the free-wilson technique to structurally related series of homologs. quantitative structure-activity relationship studies of narcotic analgetics. *Journal of Medicinal Chemistry* 20(11):1413–1419.
- Kim T, Kim Kk, Song E (2022) Selection of the most probable best. *arXiv preprint arXiv:2207.07533* .
- Ledoit O, Wolf M (2020) Analytical nonlinear shrinkage of large-dimensional covariance matrices. *The Annals of Statistics* 48(5):3043–3065.
- Li H, Lam H, Peng Y (2022) Efficient learning for clustering and optimizing context-dependent designs. *Operations Research* .
- Luo J, Hong LJ, Nelson BL, Wu Y (2015) Fully sequential procedures for large-scale ranking-and-selection problems in parallel computing environments. *Operations Research* 63(5):1177–1194.
- Mellor J, Turner J, Storkey A, Crowley EJ (2021) Neural architecture search without training. *International Conference on Machine Learning*, 7588–7598 (PMLR).
- Negoescu DM, Frazier PI, Powell WB (2011) The knowledge-gradient algorithm for sequencing experiments in drug discovery. *INFORMS Journal on Computing* 23(3):346–363.

- Ni EC, Ciocan DF, Henderson SG, Hunter SR (2017) Efficient ranking and selection in parallel computing environments. *Operations Research* 65(3):821–836.
- Pei L, Nelson BL, Hunter SR (2022) Parallel adaptive survivor selection. *Operations Research* .
- Peng Y, Chen CH, Fu MC, Hu JQ (2016) Dynamic sampling allocation and design selection. *INFORMS Journal on Computing* 28(2):195–208.
- Peng Y, Chen CH, Fu MC, Hu JQ (2017) Gradient-based myopic allocation policy: An efficient sampling procedure in a low-confidence scenario. *IEEE Transactions on Automatic Control* 63(9):3091–3097.
- Qu H, Ryzhov IO, Fu MC, Ding Z (2015) Sequential selection with unknown correlation structures. *Operations Research* 63(4):931–948.
- Rinott Y (1978) On two-stage selection procedures and related probability-inequalities. *Communications in Statistics-Theory and methods* 7(8):799–811.
- Russo D (2020) Simple bayesian algorithms for best-arm identification. *Operations Research* 68(6):1625–1647.
- Shlens J (2014) A tutorial on principal component analysis. *arXiv preprint arXiv:1404.1100* .
- Snell J, Swersky K, Zemel R (2017) Prototypical networks for few-shot learning. *Advances in neural information processing systems* 30.
- Vigneau E, Qannari E (2003) Clustering of variables around latent components. *Communications in Statistics-Simulation and Computation* 32(4):1131–1150.
- Zhong Y, Hong LJ (2022) Knockout-tournament procedures for large-scale ranking and selection in parallel computing environments. *Operations Research* 70(1):432–453.
- Zhou Y, Fu MC, Ryzhov IO (2023) Sequential learning with a similarity selection index. *Operations Research*

Online Appendices

Before starting the appendix, we first introduce some notations: $\text{PCS}(\tau) = P(\bar{x}_\tau - \bar{x}_j > 0, j \neq \tau)$. The vector $(\bar{x}_\tau - \bar{x}_1, \dots, \bar{x}_\tau - \bar{x}_p)$ has a joint normal distribution with mean $(\mu_\tau - \mu_1, \dots, \mu_\tau - \mu_p)$ and covariance matrix $\Lambda^\tau = [\Lambda_{ij}^\tau]_{(p-1) \times (p-1)}$, where $\Lambda_{ij}^\tau = \text{cov}(\bar{x}_\tau - \bar{x}_i, \bar{x}_\tau - \bar{x}_j)$, $i, j \in \mathcal{P} \setminus \{\tau\}$. $\text{PCS}(\tau)$ can be rewritten as $P(y_1^\tau > -d_1^\tau, \dots, y_p^\tau > -d_p^\tau)$, where $y_i^\tau = \frac{\bar{x}_\tau - \bar{x}_i - (\mu_\tau - \mu_i)}{\sqrt{\lambda_i^\tau}}$, $d_i^\tau = \frac{\mu_\tau - \mu_i}{\sqrt{\lambda_i^\tau}}$, and $\lambda_i^\tau = \text{var}(\bar{x}_\tau - \bar{x}_i) = \frac{\sigma_\tau^2}{N_\tau} + \frac{\sigma_i^2}{N_i} - 2 \frac{\text{cov}(X_\tau, X_i)}{\max(N_\tau, N_i)}$ ($i \in \mathcal{P} \setminus \{\tau\}$). Then $\mathbf{y}^\tau = (y_1^\tau, \dots, y_{\tau-1}^\tau, y_{\tau+1}^\tau, \dots, y_p^\tau) \sim N(0, \Phi^\tau)$ with probability density function $f_{\mathbf{y}^\tau}$. The covariance matrix is

$$\Phi^\tau = \begin{pmatrix} 1 & \cdots & \tilde{r}_{1,p}^\tau \\ \vdots & \ddots & \vdots \\ \tilde{r}_{p,1}^\tau & \cdots & 1 \end{pmatrix}_{(p-1) \times (p-1)},$$

where $\tilde{r}_{i,j}^\tau$ is the correlation coefficient between $(\bar{x}_\tau - \bar{x}_i)$ and $(\bar{x}_\tau - \bar{x}_j)$, $i, j \in \mathcal{P} \setminus \{\tau\}$. If Assumption 2 holds and p is fixed, $\Lambda_{ij}^\tau = \frac{\sigma_\tau^2}{N_\tau} + \frac{\text{cov}(X_i, X_j)}{\max(N_i, N_j)} - \frac{\text{cov}(X_\tau, X_i)}{\max(N_\tau, N_i)} - \frac{\text{cov}(X_\tau, X_j)}{\max(N_\tau, N_j)} \sim \mathcal{O}(\frac{1}{N})$ and $\lambda_i^\tau, \lambda_j^\tau \sim \mathcal{O}(\frac{1}{N})$, then we have $\tilde{r}_{i,j}^\tau \sim \mathcal{O}(1)$, meaning that its order does not increase with the growth of N .

EC.1. Proof of Theorem 1.

Proof (1) The derivative of $\text{PCS}(\tau)$ with respect to mean μ_τ is given by

$$\begin{aligned} \frac{\partial \text{PCS}(\tau)}{\partial \mu_\tau} &= \frac{\partial}{\partial \mu_\tau} P(y_1^\tau > -d_1^\tau, \dots, y_p^\tau > -d_p^\tau) \\ &= \frac{\partial}{\partial \mu_\tau} d_1^\tau \int_{-d_2}^{\infty} \cdots \int_{-d_p}^{\infty} f_{\mathbf{y}^\tau}(-d_1^\tau, y_2, \dots, y_p) dy_2 \cdots dy_p + \cdots \\ &\quad + \frac{\partial}{\partial \mu_\tau} d_p^\tau \int_{-d_1}^{\infty} \cdots \int_{-d_{p-1}}^{\infty} f_{\mathbf{y}^\tau}(y_1, y_2, \dots, -d_p^\tau) dy_1 \cdots dy_{p-1}. \end{aligned} \tag{EC.1}$$

Each term in EC.1 is bounded and $\text{PCS}(\tau)$ is differentiable at any point within the domain of μ_τ because the left and right derivatives are identical. Similarly, $\text{PCS}(\tau)$ is also differentiable with respect to μ_i for $i \in \mathcal{P} \setminus \{\tau\}$. Additionally, it is straightforward to verify that the partial derivative $\frac{\partial \text{PCS}(\tau)}{\partial \mu_i}$ ($i \in \mathcal{P}$) is continuous. Therefore, $\text{PCS}(\tau)$ is differentiable with respect to $\boldsymbol{\mu} = (\mu_1, \dots, \mu_p)$. Since $\frac{\partial d_i^\tau}{\partial \mu_\tau} > 0$ holds for any $i \in \mathcal{P} \setminus \{\tau\}$, we have $\frac{\partial \text{PCS}(\tau)}{\partial \mu_\tau} > 0$.

(2) Next, we prove that τ^* converges to [1] almost surely as $N_i \rightarrow \infty$, $\forall i \in \mathcal{P}$. For any $\tau \neq [1]$, there exists $i_0(\tau) \in \mathcal{P}$, s.t. $\mu_\tau - \mu_{i_0} < 0$. Then $d_{i_0}^\tau \rightarrow -\infty$ when $N_i \rightarrow \infty$, $\forall i \in \mathcal{P}$. Then we have

$$\text{PCS}(\tau) = P(y_1^\tau > -d_1^\tau, \dots, y_p^\tau > -d_p^\tau) \leq P(y_{i_0}^\tau > -d_{i_0}^\tau) \rightarrow 0.$$

Notice that $d_i^{[1]} \rightarrow +\infty$ for any $i \in \mathcal{P} \setminus \{[1]\}$ when $N_i \rightarrow \infty$. Therefore, $P(y_i^{[1]} > -d_i^{[1]}) \rightarrow 1$. Then we have

$$\begin{aligned} \text{PCS}([1]) &= P(y_1^{[1]} > -d_1^{[1]}, \dots, y_p^{[1]} > -d_p^{[1]}) \\ &\geq \sum_{i \in \mathcal{P} \setminus \{[1]\}} P(y_i^{[1]} > -d_i^{[1]}) - (p-2) \rightarrow p-1 - (p-2) = 1. \end{aligned}$$

Since τ^* is the one maximizing $\text{PCS}(\tau)$, $\tau^* \rightarrow [1]$ almost surely. \square

EC.2. Proof of Proposition 1.

Proof First, we consider the situation when all means are equal, i.e., $\boldsymbol{\mu} = (\mu_1, \dots, \mu_p)$ where $\mu_1 = \dots = \mu_p$. Under this parameter figuration, by Slepian normal comparison lemma (Azaïs and Wschebor 2009), for any $\tau \in \mathcal{P} \setminus \{\tau_0\}$, we have

$$\begin{aligned} &\text{PCS}(\tau; \boldsymbol{\mu}) - \text{PCS}(\tau_0; \boldsymbol{\mu}) \\ &= P(y_1^\tau > 0, \dots, y_p^\tau > 0) - P(y_1^{\tau_0} > 0, \dots, y_p^{\tau_0} > 0) \\ &\leq \frac{1}{2\pi} \sum_{1 \leq i < j \leq p} (\arcsin \tilde{r}_{i,j}^\tau - \arcsin \tilde{r}_{i,j}^{\tau_0})^+ = 0. \end{aligned}$$

Therefore, $\text{PCS}(\tau_0)$ is the maximum. According to Theorem 1, $\text{PCS}(\tau)$ is a continuous function of the mean vector. Therefore, if we modify each μ_τ ($\tau \neq \tau_0$) slightly by δ_τ to construct a new parameter figuration $\boldsymbol{\mu}' = (\mu'_1, \dots, \mu'_p)$, where $\mu'_\tau = \mu_\tau + \delta_\tau$ ($\tau \neq \tau_0$) and $\mu'_{\tau_0} = \mu_{\tau_0}$, there exists a $\delta > 0$, s.t. if $|\delta_\tau| < \delta$ holds for any $\tau \neq \tau_0$, then

$$|\text{PCS}(\tau; \boldsymbol{\mu}') - \text{PCS}(\tau; \boldsymbol{\mu})| < \frac{1}{2}(\text{PCS}(\tau_0; \boldsymbol{\mu}) - \text{PCS}(\tau; \boldsymbol{\mu})),$$

and

$$|\text{PCS}(\tau_0; \boldsymbol{\mu}') - \text{PCS}(\tau_0; \boldsymbol{\mu})| < \frac{1}{2}(\text{PCS}(\tau_0; \boldsymbol{\mu}) - \text{PCS}(\tau; \boldsymbol{\mu})).$$

Then we have

$$\begin{aligned}
& \text{PCS}(\tau_0; \boldsymbol{\mu}') - \text{PCS}(\tau; \boldsymbol{\mu}') = \text{PCS}(\tau_0; \boldsymbol{\mu}) + \text{PCS}(\tau_0; \boldsymbol{\mu}') - \text{PCS}(\tau_0; \boldsymbol{\mu}) \\
& \quad - [\text{PCS}(\tau; \boldsymbol{\mu}) + \text{PCS}(\tau; \boldsymbol{\mu}') - \text{PCS}(\tau; \boldsymbol{\mu})] \\
& > \text{PCS}(\tau_0; \boldsymbol{\mu}) - \text{PCS}(\tau; \boldsymbol{\mu}) - 2 \times \frac{1}{2} \times (\text{PCS}(\tau_0; \boldsymbol{\mu}) - \text{PCS}(\tau; \boldsymbol{\mu})) = 0.
\end{aligned}$$

$\text{PCS}(\tau_0)$ is still the maximum. $\tau^* = \tau_0$. \square

EC.3. Proof of Theorem 2, Corollary 1 and Lemma 1.

Here, we prove a more general result that encompasses not only the derivative of PCS with respect to the correlation information but also the derivative with respect to variance information.

(a) $\frac{\partial \text{PCS}(\tau)}{\partial \sigma_\tau} = I^+ + I^- + E$, where $I^+ = \sum_{i \in \mathcal{I}^+} I_i$, $I^- = \sum_{j \in \mathcal{I}^-} I_j$, and the term $I_i > 0$ for $i \in \mathcal{I}^+(\tau)$, $I_j < 0$ for $j \in \mathcal{I}^-(\tau)$;

(b) **Theorem 2:** $\forall i \in \mathcal{P} \setminus \{\tau\}$, $\frac{\partial \text{PCS}(\tau)}{\partial r_{i\tau}} = \tilde{I}_i + \tilde{E}_i$, where $\tilde{I}_i > 0$ for $i \in \mathcal{I}^-(\tau)$ and < 0 for $i \in \mathcal{I}^+(\tau)$;

(c) **Lemma 1:** $\forall i, j \in \mathcal{P} \setminus \{\tau\}$, $\frac{\partial \text{PCS}(\tau)}{\partial r_{ij}} \geq 0$. If Assumption 3 holds, then $\frac{\partial \text{PCS}(\tau)}{\partial r_{ij}} \sim o\left(\left|\frac{\partial \text{PCS}(\tau)}{\partial r_{i\tau}}\right|\right)$.

The symbols in the appendix differ slightly from those in the main text. The symbols I_i and E_i in the main text correspond to \tilde{I}_i and \tilde{E}_i here. The proof of Corollary 1 is embedded in (b).

Proof (a) The derivative of $\text{PCS}(\tau)$ with respect to the variance of τ is given by

$$\begin{aligned}
\frac{\partial \text{PCS}(\tau)}{\partial \sigma_\tau} &= \frac{\partial P(y_1^\tau > -d_1^\tau, \dots, y_p^\tau > -d_p^\tau)}{\partial \sigma_\tau} \\
&= \frac{\partial d_1^\tau}{\partial \sigma_\tau} \int_{-d_2}^{\infty} \cdots \int_{-d_p}^{\infty} f_{y^\tau}(-d_1^\tau, y_2, \dots, y_p) dy_2 \cdots dy_p + \cdots \\
&+ \frac{\partial d_p^\tau}{\partial \sigma_\tau} \int_{-d_1}^{\infty} \cdots \int_{-d_{p-1}}^{\infty} f_{y^\tau}(y_1, y_2, \dots, -d_p^\tau) dy_1 \cdots dy_{p-1} \\
&+ 2 \sum_{1 \leq i < j \leq p, i, j \neq \tau} \frac{\partial \text{PCS}(\tau)}{\partial \tilde{r}_{i,j}^\tau} \frac{\partial \tilde{r}_{i,j}^\tau}{\partial \sigma_\tau} \\
&= I^+ - I^- + E,
\end{aligned} \tag{EC.2}$$

where

$$\begin{aligned}
I^+ &\triangleq \sum_{i \in \mathcal{P} \setminus \{\tau\}} \max\{0, I_i^\tau\}, \\
I^- &\triangleq \sum_{i \in \mathcal{P} \setminus \{\tau\}} \min\{0, I_i^\tau\},
\end{aligned}$$

$$I_i^\tau \triangleq \frac{\partial d_i^\tau}{\partial \sigma_\tau} \int_{-d_1^\tau}^\infty \cdots \int_{-d_{i-1}^\tau}^\infty \int_{-d_{i+1}^\tau}^\infty \cdots \int_{-d_{\tau-1}^\tau}^\infty \int_{-d_{\tau+1}^\tau}^\infty \cdots \int_{-d_p^\tau}^\infty f_{y^\tau}(y_1, \dots, -d_i^\tau, \dots, y_p) dy_1 \cdots dy_p,$$

$$E = 2 \sum_{1 \leq i < j \leq p, i, j \neq \tau} \frac{\partial \text{PCS}(\tau)}{\partial \tilde{r}_{i,j}^\tau} \frac{\partial \tilde{r}_{i,j}^\tau}{\partial \sigma_\tau}. \quad (\text{EC.3})$$

I^+ is the sum of the positive parts of I_i^τ ($i \in \mathcal{P} \setminus \{\tau\}$) and I^- is the sum of negative parts of them.

I_i^τ depends on τ , but for simplicity, we omit τ and use I_i instead.

Notice that $d_i^\tau = \frac{\mu_\tau - \mu_i}{\sqrt{\lambda_i^\tau}}$ is not necessarily non-negative as μ_τ does not always exceed μ_i . If $i \in \mathcal{I}^+(\tau) \triangleq \{i | \mu_i > \mu_\tau, i \in \mathcal{P} \setminus \{\tau\}\}$, $\frac{\partial d_i^\tau}{\partial \sigma_\tau} > 0$, the term $I_i > 0$, which will only contribute to I^+ . Conversely, if $j \in \mathcal{I}^-$, the term $I_j < 0$ and it is only accounted for in I^- . This means that $I^+ = \sum_{i \in \mathcal{I}^+} I_i$ and $I^- = \sum_{i \in \mathcal{I}^-} |I_i|$.

In the following part, we will evaluate the growth rate of the terms I_i and E as the total sample size N increases. First, we prove that $\frac{\partial \text{PCS}(\tau)}{\partial \tilde{r}_{i,j}^\tau}$ is bounded. With Slepian normal comparison lemma, we have

$$0 \leq \frac{\text{PCS}(\tau; \tilde{r}_{i,j}^\tau + \delta) - \text{PCS}(\tau; \tilde{r}_{i,j}^\tau)}{\delta}$$

$$\leq \frac{\arcsin(\tilde{r}_{i,j}^\tau + \delta) - \arcsin(\tilde{r}_{i,j}^\tau)}{2\pi\delta} \times \exp\left(-\frac{(d_i^\tau)^2 + (d_j^\tau)^2}{2(1 + \max\{|\arcsin(\tilde{r}_{i,j}^\tau + \delta)|, \arcsin(\tilde{r}_{i,j}^\tau)\})}\right).$$

Let $\delta \rightarrow 0$, then

$$0 \leq \frac{\partial \text{PCS}(\tau)}{\partial \tilde{r}_{i,j}^\tau} \leq \frac{1}{2\pi\sqrt{1 - (\tilde{r}_{i,j}^\tau)^2}} \exp\left(-\frac{(d_i^\tau)^2 + (d_j^\tau)^2}{2(1 + \arcsin(\tilde{r}_{i,j}^\tau))}\right). \quad (\text{EC.4})$$

According to Assumption 2, we have $N_i \sim \mathcal{O}(N)$, $\forall i \in \mathcal{P}$ (p is fixed). Then $d_i^\tau =$

$$\frac{\mu_\tau - \mu_i}{\sqrt{\frac{\sigma_\tau^2}{N_\tau} + \frac{\sigma_i^2}{N_i} - 2\frac{\text{cov}(X_\tau, X_i)}{\max(N_\tau, N_i)}}} \sim \mathcal{O}(\sqrt{N}) \text{ and } \tilde{r}_{i,j}^\tau \sim \mathcal{O}(1). \text{ Then}$$

$$\frac{\partial \text{PCS}(\tau)}{\partial \tilde{r}_{i,j}^\tau} \sim \mathcal{O}\left(\exp\left(-\frac{(d_i^\tau)^2 + (d_j^\tau)^2}{2(1 + \arcsin(\tilde{r}_{i,j}^\tau))}\right)\right),$$

and we can introduce a positive constant B_{ij} such that $\frac{\partial \text{PCS}(\tau)}{\partial \tilde{r}_{i,j}^\tau} \sim \mathcal{O}(e^{-B_{ij}N})$.

We define

$$B_i = \min_{j \neq i} B_{ij},$$

$$B = \min_{i \in \mathcal{P} \setminus \{\tau\}} B_i.$$

It is straightforward to verify that $\frac{\partial \tilde{r}_{i,j}^\tau}{\partial \sigma_\tau} \sim \mathcal{O}(1)$ by definition. Then with (EC.3), we have

$$E \sim \mathcal{O}\left(\exp\left(-\min_{i,j \in \mathcal{P} \setminus \{\tau\}} \frac{(d_i^\tau)^2 + (d_j^\tau)^2}{2(1 + \arcsin(\tilde{r}_{i,j}^\tau))}\right)\right) \sim \mathcal{O}(e^{-BN}). \quad (\text{EC.5})$$

Then, by definition, we have

$$\frac{\partial d_i^\tau}{\partial \sigma_\tau} \sim \mathcal{O}(\sqrt{N}). \quad (\text{EC.6})$$

Next, we will evaluate the following integral for each $i \in \mathcal{P} \setminus \{\tau\}$:

$$\begin{aligned} \frac{I_i^\tau}{\frac{\partial d_i^\tau}{\partial \sigma_\tau}} &= \int_{-d_1^\tau}^\infty \cdots \int_{-d_{i-1}^\tau}^\infty \int_{-d_{i+1}^\tau}^\infty \cdots \int_{-d_{\tau-1}^\tau}^\infty \int_{-d_{\tau+1}^\tau}^\infty \cdots \int_{-d_p^\tau}^\infty f_{y^\tau}(y_1, \dots, -d_i^\tau, \dots, y_p) dy_1 \cdots dy_p \\ &= f_{y_i^\tau}(-d_i^\tau) \int_{-d_1^\tau}^\infty \cdots \int_{-d_{i-1}^\tau}^\infty \int_{-d_{i+1}^\tau}^\infty \cdots \int_{-d_{\tau-1}^\tau}^\infty \int_{-d_{\tau+1}^\tau}^\infty \cdots \int_{-d_p^\tau}^\infty f_{y^\tau|y_i^\tau}(y_1, \dots, y_p) dy_1 \cdots dy_p. \end{aligned} \quad (\text{EC.7})$$

$f_{y_i^\tau}$ is the marginal density of y_i^τ , which is standard normal, and $f_{y^\tau|y_i^\tau}$ is the conditional density of y^τ given y_i^τ , which is a multivariate normal distribution $N(\tilde{\mu}_i, \tilde{\Sigma}_i)$ of dimension $p-2$ with mean and covariance given by

$$\tilde{\mu}_i = (-d_i^\tau \tilde{r}_{i,1}^\tau, \dots, -d_i^\tau \tilde{r}_{i,p}^\tau), \quad (\text{EC.8})$$

$$\tilde{\Sigma}_i = \begin{pmatrix} 1 - (\tilde{r}_{i,1}^\tau)^2 & \tilde{r}_{1,2}^\tau - \tilde{r}_{i,1}^\tau \tilde{r}_{i,2}^\tau & \cdots & \tilde{r}_{1,p}^\tau - \tilde{r}_{i,1}^\tau \tilde{r}_{i,p}^\tau \\ \tilde{r}_{2,1}^\tau - \tilde{r}_{i,2}^\tau \tilde{r}_{i,1}^\tau & 1 - (\tilde{r}_{i,2}^\tau)^2 & \cdots & \tilde{r}_{2,p}^\tau - \tilde{r}_{i,2}^\tau \tilde{r}_{i,p}^\tau \\ \vdots & \vdots & \ddots & \vdots \\ \tilde{r}_{p,1}^\tau - \tilde{r}_{i,p}^\tau \tilde{r}_{i,1}^\tau & \cdots & \cdots & 1 - (\tilde{r}_{i,p}^\tau)^2 \end{pmatrix}_{(p-2) \times (p-2)}. \quad (\text{EC.9})$$

By transforming variables, we have

$$\begin{aligned} &\int_{-d_1^\tau}^\infty \cdots \int_{-d_p^\tau}^\infty f_{y^\tau|y_i^\tau=-d_i^\tau}(y_1, \dots, y_p) dy_1 \cdots dy_p \\ &= \int_{-\tilde{d}_1^\tau}^\infty \cdots \int_{-\tilde{d}_p^\tau}^\infty f_Z(z_1, \dots, z_p) dz_1 \cdots dz_p, \end{aligned} \quad (\text{EC.10})$$

where $-\tilde{d}_j^\tau = -d_j^\tau + d_i^\tau \tilde{r}_{i,j}^\tau$ and f_Z is the density of a multivariate normal distribution with zero mean and covariance matrix $\Sigma^Z = \tilde{\Sigma}_i$. Then, the integral (EC.10) is rewritten as

$$\begin{aligned} &P_Z(z_j > -\tilde{d}_j^\tau, j \in \mathcal{P} \setminus \{i, \tau\}) \\ &= P_Z(\{z_r > -\tilde{d}_r^\tau, r \in \mathcal{S}_i^+(\tau)\} \cap \{z_s > -\tilde{d}_s^\tau, s \in \mathcal{S}_i^-(\tau)\}) \\ &\leq \min\{P_Z(z_r > -\tilde{d}_r^\tau, r \in \mathcal{S}_i^+(\tau)), P_Z(z_s > -\tilde{d}_s^\tau, s \in \mathcal{S}_i^-(\tau))\}, \end{aligned} \quad (\text{EC.11})$$

where $\mathcal{S}_{-i}^+(\tau) \triangleq \{r \in \mathcal{P} \setminus \{i, \tau\} \mid -\tilde{d}_r^\tau > 0\}$ and $\mathcal{S}_{-i}^-(\tau) \triangleq \{s \in \mathcal{P} \setminus \{i, \tau\} \mid -\tilde{d}_s^\tau < 0\}$.

Next we evaluate the two terms within the ‘‘min’’ operator respectively. The term

$$P_Z(z_s > -\tilde{d}_s^\tau, s \in \mathcal{S}_{-i}^-(\tau)) \geq P_Z(z_s > 0, s \in \mathcal{S}_{-i}^-(\tau))$$

is lower bounded by a positive value that will not reduce to 0 as N increases. However, the other term $P_Z(z_r > -\tilde{d}_r^\tau, r \in \mathcal{S}_{-i}^+(\tau))$ will reduce to 0 as N grows since $d_r^\tau \sim \mathcal{O}(\sqrt{N})$. Next we evaluate the rate of convergence to 0. With Hashorva and Hüsler (2003), we have

$$P_Z(z_r > -\tilde{d}_r^\tau, r \in \mathcal{S}_{-i}^+(\tau)) \sim \mathcal{O}\left(\exp\left(-\frac{\langle \mathbf{d}_S, (\Sigma_S^Z)^{-1} \mathbf{d}_S \rangle}{2}\right) \prod_{r \in S} h_r^{-1}\right), \quad (\text{EC.12})$$

where $\mathbf{d} = (-\tilde{d}_1^\tau, \dots, -\tilde{d}_p^\tau) \in \mathbb{R}^{p-2}$, $h_r \sim \mathcal{O}(\sqrt{N})$ is the r -th element of $(\Sigma_S^Z)^{-1} \mathbf{d}_S$, S is a subset of $\mathcal{S}_{-i}^+(\tau)$. For simplicity, we omit the term $\prod_{r \in S} h_r^{-1}$, as it does not affect the comparisons of exponentially decaying terms. Then

$$P_Z(z_r > -\tilde{d}_r^\tau, r \in \mathcal{S}_{-i}^+(\tau)) \sim \mathcal{O}\left(\exp\left(-\frac{\langle \mathbf{d}_S, (\Sigma_S^Z)^{-1} \mathbf{d}_S \rangle}{2}\right)\right). \quad (\text{EC.13})$$

Therefore, with (EC.7), (EC.11) and (EC.13), we have

$$I_i^\tau \sim \mathcal{O}\left(\frac{\partial d_i^\tau}{\partial \sigma_\tau} f_{y_i^\tau}(-d_i^\tau) \exp\left(-\frac{\langle \mathbf{d}_S, (\Sigma_S^Z)^{-1} \mathbf{d}_S \rangle}{2}\right)\right) = \mathcal{O}\left(\sqrt{N} \exp\left(-\frac{\langle \mathbf{d}_S, (\Sigma_S^Z)^{-1} \mathbf{d}_S \rangle + (d_i^\tau)^2}{2}\right)\right).$$

To simplify the form, we rewrite the quadratic form by introducing $A_i > 0$ such that

$$I_i^\tau \sim \mathcal{O}(\sqrt{N} e^{-A_i N}). \quad (\text{EC.14})$$

(b) Similar to (a), the derivative of PCS (τ) with respect to correlation information $\{r_{\tau, i}\}$ is given

by

$$\begin{aligned} \frac{\partial \text{PCS}(\tau)}{\partial r_{\tau i}} &= \frac{\partial P(y_1^\tau > -d_1^\tau, \dots, y_p^\tau > -d_p^\tau)}{\partial r_{\tau i}} \\ &= \frac{\partial d_i^\tau}{\partial r_{\tau i}} \int_{-d_1^\tau}^\infty \cdots \int_{-d_{i-1}^\tau}^\infty \int_{-d_{i+1}^\tau}^\infty \cdots \int_{-d_p^\tau}^\infty f_{y^\tau}(y_1, \dots, -d_i^\tau, \dots, y_p) dy_1 \cdots dy_p \\ &\quad + 2 \sum_{j \in \{1, \dots, p-1\} \setminus \{i\}} \frac{\partial \text{PCS}(\tau)}{\partial \tilde{r}_{i, j}^\tau} \frac{\partial \tilde{r}_{i, j}^\tau}{\partial r_{\tau i}} \\ &= \tilde{I}_i + \tilde{E}_i, \end{aligned} \quad (\text{EC.15})$$

where

$$\begin{aligned} \tilde{I}_i &= \frac{\partial d_i^\tau}{\partial r_{\tau i}} \int_{-d_1^\tau}^{\infty} \cdots \int_{-d_{i-1}^\tau}^{\infty} \int_{-d_{i+1}^\tau}^{\infty} \cdots \int_{-d_p^\tau}^{\infty} f_{y^\tau}(y_1, \dots, -d_i^\tau, \dots, y_p) dy_1 \cdots dy_p, \\ \tilde{E}_i &= 2 \sum_{j \in \{1, \dots, p-1\} \setminus \{i\}} \frac{\partial \text{PCS}(\tau)}{\partial \tilde{r}_{i,j}^\tau} \frac{\partial \tilde{r}_{i,j}^\tau}{\partial r_{\tau i}}. \end{aligned} \quad (\text{EC.16})$$

Similar to (a), we have

$$\begin{aligned} \frac{\partial d_i^\tau}{\partial r_{\tau i}} &\sim \mathcal{O}(\sqrt{N}), \\ \tilde{I}_i &\sim \mathcal{O}\left(\sqrt{N} \cdot \exp\left(-\frac{\mathbf{d}_S^\tau (\Sigma_S^Z)^{-1} \mathbf{d}_S^\tau + (d_i^\tau)^2}{2}\right)\right) \sim \mathcal{O}(\sqrt{N} e^{-A_i N}), \end{aligned}$$

and

$$\begin{aligned} \frac{\partial \tilde{r}_{i,j}^\tau}{\partial r_{\tau i}} &\sim \mathcal{O}(1), \\ \tilde{E}_i &\sim \mathcal{O}\left(\exp\left(-\min_{j \neq i} \frac{(d_i^\tau)^2 + (d_j^\tau)^2}{2(1 + \arcsin(\tilde{r}_{i,j}^\tau))}\right)\right) \sim \mathcal{O}(e^{-B_i N}). \end{aligned}$$

(c) $\forall i, j \in \mathcal{P} \setminus \{\tau\}$, since d_i^τ and d_j^τ are independent of r_{ij} , we have

$$\begin{aligned} \frac{\partial \text{PCS}(\tau)}{\partial r_{ij}} &= \frac{\partial P(y_1^\tau > -d_1^\tau, \dots, y_p^\tau > -d_p^\tau)}{\partial r_{ij}} \\ &= 2 \cdot \frac{\partial \text{PCS}(\tau)}{\partial \tilde{r}_{i,j}^\tau} \frac{\partial \tilde{r}_{i,j}^\tau}{\partial r_{ij}}. \end{aligned} \quad (\text{EC.17})$$

It is easy to verify that $\frac{\partial \tilde{r}_{i,j}^\tau}{\partial r_{ij}} > 0$ and according to (EC.4), $\frac{\partial \text{PCS}(\tau)}{\partial \tilde{r}_{i,j}^\tau} \geq 0$. Therefore, $\frac{\partial \text{PCS}(\tau)}{\partial r_{ij}} \geq 0$.

As for the order of magnitude, we have $\frac{\partial \text{PCS}(\tau)}{\partial r_{ij}} \sim \mathcal{O}(e^{-B_{ij} N})$. If Assumption 3 holds, $B_{ij} \geq B_i > A_i$, then we have $|\frac{\partial \text{PCS}(\tau)}{\partial r_{ij}}| \sim o(\frac{\partial \text{PCS}(\tau)}{\partial r_{i\tau}})$ ($i, j \neq \tau$). The influence of $\frac{\partial \text{PCS}(\tau)}{\partial r_{ij}}$ is negligible compared to $\frac{\partial \text{PCS}(\tau)}{\partial r_{i\tau}}$. \square

EC.4. Proof of Theorem 3 and the Order of γ in (4).

Proof We view $\text{PCS}(\tau; \Sigma, N)$ as a function of the total sample size and correlation matrix. First, we consider the strategy \mathcal{R} : randomly assigning $\frac{p}{k}$ alternatives to each processor. In the following analysis, we focus on calculating the expected sample complexity reduction for the first processor. By symmetry, multiplying the result by k gives the total sample complexity reduction. The index set of alternatives in the first processor is denoted as \mathcal{P}_1 . The local best τ_1 of this processor is

assumed to be from cluster \mathcal{G}_1 . In this processor, besides τ_1 , there are η alternatives from cluster \mathcal{G}_1 (the index set of those alternatives is denoted as $\mathcal{J}_1 \subseteq \mathcal{P}_1$). The remaining $\frac{p}{k} - \eta$ alternatives are from other clusters. η follows a hypergeometric distribution $H(p, \frac{p}{k}, \frac{p}{k})$ and $E(\eta) = \frac{(\frac{p}{k})^2}{p}$. The covariance matrix of alternatives in this processor is Σ . Suppose the initialization sample size is N_0 and the corresponding $\text{PCS}(\tau_1; \Sigma, N_0)$ of this processor is $1 - \alpha_0$ at this point. We continue sampling until PCS reaches $1 - \alpha$. The sample size is increased to N_R . According to mean value theorem,

$$\text{PCS}(\tau_1; \Sigma, N_R) - \text{PCS}(\tau_1; \Sigma, N_0) = \frac{\partial \text{PCS}(\tau_1; \Sigma, N_0 + \xi_R(N_R - N_0))}{\partial N} \cdot (N_R - N_0) = \alpha_0 - \alpha, \quad (\text{EC.18})$$

where $\xi_R \in (0, 1)$. This process is illustrated in the red line in Figure EC.1.

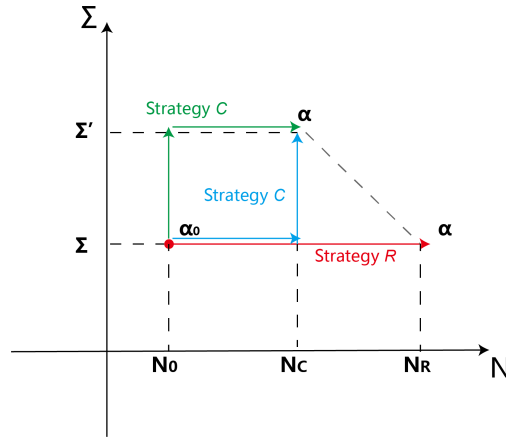


Figure EC.1 Starting from the initialization, Strategy \mathcal{R} directly increases the total sample size, while Strategy \mathcal{C} is equivalent to first increasing the total sample size and then changing the covariance.

Next we consider the strategy \mathcal{C} . By using correlation-based clustering, $\beta(\frac{p}{k})$ alternatives in the first processor are correctly clustered (i.e., from \mathcal{G}_1), where $\beta = \frac{\sum_{i \in \mathcal{P}_1 \setminus \{\tau_1\}} \mathbb{I}(G_n(i) = G(i))}{\frac{p}{k}}$ and n is the sample size used for learning correlation information. Since $\text{PCC} = P(\Pi_n = \Pi) \leq P(G_n(i) = G(i))$, $\forall i \in \mathcal{P}_1$, and the cardinality $|\mathcal{P}_1 \setminus \{\tau_1\}| = \frac{p}{k}$, we have

$$E(\beta) = E\left(\frac{\sum_{i \in \mathcal{P}_1 \setminus \{\tau_1\}} \mathbb{I}(G_n(i) = G(i))}{\frac{p}{k}}\right) = \frac{\sum_{i \in \mathcal{P}_1 \setminus \{\tau_1\}} P(G_n(i) = G(i))}{\frac{p}{k}} \geq \frac{\frac{p}{k} \cdot \text{PCC}}{\frac{p}{k}} = \text{PCC}. \quad (\text{EC.19})$$

The transition from Strategy \mathcal{R} to Strategy \mathcal{C} is equivalent to increasing the number of alternatives belonging to cluster \mathcal{G}_1 from η to $\beta(\frac{p}{k})$. Furthermore, this is equivalent to changing the correlation structure of this processor from Σ to Σ' while keeping the means and variances unchanged. Specifically, the change in the correlation structure is as follows:

(i) The correlation coefficients between $\beta(\frac{p}{k}) - \eta$ alternatives in $\mathcal{P}_1 \setminus \mathcal{J}_1$ and alternative τ_1 are increased by Δr (the index set of those $\beta(\frac{p}{k}) - \eta$ alternatives is denoted as \mathcal{J}_2). For simplifying calculations, we assume that among the remaining $\mathcal{J}_3 \triangleq \mathcal{P}_1 \setminus (\mathcal{J}_1 \cup \mathcal{J}_2 \cup \{\tau_1\})$, there are no alternatives belonging to the same cluster as \mathcal{J}_2 . This is reasonable, because according to Lemma 1, the impact of the correlation between \mathcal{J}_2 and \mathcal{J}_3 is a negligible lower-order term. (ii) As for the correlation coefficients $\{r_{i,j}\}_{i,j \in \mathcal{P}_1 \setminus \{\tau_1\}}$ between two alternatives in $\mathcal{P}_1 \setminus \{\tau_1\}$, $\eta[\beta(\frac{p}{k}) - \eta]$ of them are increased by Δr (i.e., the correlations between the alternatives in \mathcal{J}_1 and \mathcal{J}_2). The remaining correlation coefficients remain unchanged.

Starting from the initialization N_0 samples, we continue sampling until PCS reaches $1 - \alpha$ and the total sample size is N_C . This process is depicted by the green line in Figure EC.1, where the correlation structure is first altered to Σ' , and then the total sample size is increased to N_C . This process is equivalent to the one illustrated by the blue line in Figure EC.1, which involves first increasing total sample size, keeping the correlation coefficients constant and then altering the correlation structure. Then by mean value theorem,

$$\begin{aligned} & \text{PCS}(\tau_1; \Sigma', N_C) - \text{PCS}(\tau_1; \Sigma, N_0) \\ &= \frac{\partial \text{PCS}(\tau_1)}{\partial N} \cdot (N_C - N_0) + \sum_{i \in \mathcal{J}_2} \frac{\partial \text{PCS}(\tau_1)}{\partial r_{i,\tau_1}} \Delta r + \sum_{i \in \mathcal{J}_1, j \in \mathcal{J}_2} \frac{\partial \text{PCS}(\tau_1)}{\partial r_{ij}} \Delta r \\ &= \alpha_0 - \alpha, \end{aligned} \tag{EC.20}$$

where $\frac{\partial \text{PCS}(\tau_1)}{\partial N}$ is evaluated at a point $(\Sigma, N_0 + \xi_C(N_C - N_0))$ and $\xi_C \in (0, 1)$. $\frac{\partial \text{PCS}(\tau_1)}{\partial r_{i,\tau_1}}$ and $\frac{\partial \text{PCS}(\tau_1)}{\partial r_{ij}}$ are evaluated at a point $(\Sigma + \xi'(\Sigma' - \Sigma), N_0 + \xi_C(N_C - N_0))$, where $\xi' \in (0, 1)$.

With Lemma 1, we have

$$\sum_{i \in \mathcal{J}_1, j \in \mathcal{J}_2} \frac{\partial \text{PCS}(\tau_1)}{\partial r_{ij}} \Delta r > 0. \tag{EC.21}$$

Since each P-OS has maximum mean, according to Theorem 2 and Assumption 3, $\frac{\partial \text{PCS}(\tau_1)}{\partial r_{i,\tau_1}} \geq 0$ for any $i \neq \tau_1$, if we omit lower-order terms. As shown in Figure EC.1, the process of strategy \mathcal{R} and \mathcal{C} have the same starting (α_0) and ending points (α). With EC.18 and EC.20, the identical $\alpha_0 - \alpha$ terms are canceled out, then we have

$$\begin{aligned} \sum_{i \in \mathcal{J}_2} \frac{\partial \text{PCS}(\tau_1)}{\partial r_{i,\tau_1}} \Delta r &\leq \sum_{i \in \mathcal{J}_2} \frac{\partial \text{PCS}(\tau_1)}{\partial r_{i,\tau_1}} \Delta r + \sum_{i \in \mathcal{J}_1, j \in \mathcal{J}_2} \frac{\partial \text{PCS}(\tau_1)}{\partial r_{ij}} \Delta r \\ &= \frac{\partial \text{PCS}(\tau_1; \Sigma, N_0 + \xi_R(N_R - N_0))}{\partial N} \cdot (N_R - N_0) - \\ &\quad \frac{\partial \text{PCS}(\tau_1; \Sigma, N_0 + \xi_C(N_C - N_0))}{\partial N} \cdot (N_C - N_0) \\ &\leq \frac{\partial \text{PCS}(\tau_1; \Sigma, N_0 + \xi_C(N_C - N_0))}{\partial N} \cdot (N_R - N_C) \end{aligned}$$

The “ \leq ” in the last line arises because the PCS is a concave function that is increasing with respect to N , and $N_R \geq N_C$, thus $\frac{\partial \text{PCS}(\tau_1; \Sigma, N_0 + \xi_R(N_R - N_0))}{\partial N} \leq \frac{\partial \text{PCS}(\tau_1; \Sigma, N_0 + \xi_C(N_C - N_0))}{\partial N}$. Then, we have

$$(N_R - N_C) \geq \frac{\sum_{i \in \mathcal{J}_2} \frac{\partial \text{PCS}(\tau_1)}{\partial r_{i,\tau_1}} \Delta r}{\frac{\partial \text{PCS}(\tau_1; \Sigma, N_0 + \xi_C(N_C - N_0))}{\partial N}},$$

where

$$\sum_{i \in \mathcal{J}_2} \frac{\partial \text{PCS}(\tau_1)}{\partial r_{i,\tau_1}} \Delta r \geq \left(\beta \left(\frac{p}{k}\right) - \eta\right) \min_{i \in \mathcal{J}_2} \frac{\partial \text{PCS}(\tau_1)}{\partial r_{i,\tau_1}} \Delta r.$$

The derivative $\frac{\partial \text{PCS}(\tau_1)}{\partial r_{i,\tau_1}}$ is evaluated at $(\Sigma + \xi'(\Sigma' - \Sigma), N_0 + \xi_C(N_C - N_0))$. By symmetry, for any $i \in \mathcal{J}_2$, $\frac{\partial \text{PCS}(\tau_1; \Sigma + \xi'(\Sigma' - \Sigma), N_0 + \xi_C(N_C - N_0))}{\partial r_{i,\tau_1}}$ are the same. Then

$$E(N_R - N_C) \geq \frac{\frac{\partial \text{PCS}(\tau_1; \Sigma + \xi'(\Sigma' - \Sigma), N_0 + \xi_C(N_C - N_0))}{\partial r_{i_0, \tau_1}}}{\frac{\partial \text{PCS}(\tau_1; \Sigma, N_0 + \xi_C(N_C - N_0))}{\partial N}} \Delta r \left(\frac{E(\beta) - \frac{1}{k}}{k} \right) p,$$

where $i_0 \in \mathcal{J}_2$. This is the sample savings on one processor. We scale up the result by k to obtain the total sample savings for all k processors:

$$\begin{aligned} E(N_R - N_C) &\geq \frac{\frac{\partial \text{PCS}(\tau_1; \Sigma + \xi'(\Sigma' - \Sigma), N_0 + \xi_C(N_C - N_0))}{\partial r_{i_0, \tau_1}}}{\frac{\partial \text{PCS}(\tau_1; \Sigma, N_0 + \xi_C(N_C - N_0))}{\partial N}} \Delta r \left(E(\beta) - \frac{1}{k} \right) p \\ &= \gamma \Delta r \left(E(\beta) - \frac{1}{k} \right) p \geq \gamma \Delta r \left(PCC - \frac{1}{k} \right) p. \end{aligned}$$

The “ \geq ” in the last line is due to (EC.19). The proof of Theorem 3 concludes here. Next, we prove that the condition “ γ is at least $\mathcal{O}(1)$ ” is met for sampling strategies with lowest sample size growth rate $\mathcal{O}(p)$. According to Theorem 2 and Corollary 1, we have

$$\frac{\partial \text{PCS}(\tau_1)}{\partial r_{i,\tau_1}} = \tilde{I}_i + o(\tilde{I}_i). \quad (\text{EC.22})$$

Taking the derivative of PCS with respect to individual sample size N_i , we have (refer to the proof of Proposition 3 for details)

$$\frac{\partial \text{PCS}(\tau_1)}{\partial N_i} = I'_i + o(I'_i), \quad (\text{EC.23})$$

$$I'_i = \frac{\partial d_i^{\tau_1}}{\partial N_i} \int_{-d_1^{\tau_1}}^{\infty} \cdots \int_{-d_{i-1}^{\tau_1}}^{\infty} \int_{-d_{i+1}^{\tau_1}}^{\infty} \cdots \int_{-d_p^{\tau_1}}^{\infty} f_{y^{\tau_1}}(y_1, \dots, -d_i^{\tau_1}, \dots, y_p) dy_1 \cdots dy_p. \quad (\text{EC.24})$$

For any sampling strategy with lowest growth rate of total sample size $N \sim \mathcal{O}(p)$, according to Assumption 2 (all p alternatives have the same order), we can easily conclude that $N_i \sim \mathcal{O}(1)$, $\forall i \in \mathcal{P}$. With (EC.16) and (EC.24), it is straightforward to verify

$$I'_i \sim \tilde{I}_i \sim \mathcal{O}(1). \quad (\text{EC.25})$$

Therefore, with EC.22, EC.23 and EC.25, we have

$$\frac{\partial \text{PCS}(\tau_1)}{\partial r_{i,\tau_1}} \sim \frac{\partial \text{PCS}(\tau_1)}{\partial N_i} \sim \mathcal{O}(1). \quad (\text{EC.26})$$

Given Assumption 2, there exists $\omega_i \in (0, 1)$, such that $N_i = \omega_i N$, $\forall i \in \mathcal{P}$, then, according to the chain rule,

$$\frac{\partial \text{PCS}(\tau_1)}{\partial N} = \frac{\frac{\partial \text{PCS}(\tau_1)}{\partial N_i}}{\frac{\partial N}{\partial N_i}} = \omega_i \frac{\partial \text{PCS}(\tau_1)}{\partial N_i} < \frac{\partial \text{PCS}(\tau_1)}{\partial N_i}.$$

Therefore, with (EC.26), $\frac{\partial \text{PCS}(\tau_1)}{\partial N}$ is *at most* $\mathcal{O}(1)$. Then we can conclude that γ is at least $\mathcal{O}(1)$.

□

EC.5. Computation of $PCC_{\mathcal{AC}}$ and Proof of Proposition 2

In this section, we calculate the PCC of the \mathcal{AC} algorithm and present the proof of Proposition 2.

Finally, we discuss the required sample size for achieving a given clustering precision.

First, we calculate the $PCC_{\mathcal{AC}}$. Consider the following partition of the correlation matrix:

$$\Sigma = \begin{pmatrix} \Sigma_{11} & \Sigma_{12} & \cdots & \Sigma_{1k} \\ \Sigma_{12} & \Sigma_{22} & \cdots & \Sigma_{2k} \\ \vdots & \vdots & \ddots & \vdots \\ \Sigma_{1k} & \Sigma_{12} & \cdots & \Sigma_{kk} \end{pmatrix}, \quad (\text{EC.27})$$

where diagonal block Σ_{jj} ($j \in \{1, \dots, k\}$) is the $p_j \times p_j$ correlation matrix of cluster \mathcal{G}_j , and off-diagonal block Σ_{ij} ($i \neq j$) is the $p_i \times p_j$ correlation matrix between \mathcal{G}_i and \mathcal{G}_j . According to Assumption 1, each element in Σ_{jj} ($j \in \{1, \dots, k\}$) should be greater than the elements in Σ_{ij} ($i \neq j$). Accurate clustering necessitates a sufficiently precise estimation of the correlation matrix to correctly identify this relationship. We define $\Gamma = \{(ab, ac) | G(a) = G(b), G(a) \neq G(c), a, b, c \in \mathcal{P}, a \neq b\}$ and $\Gamma' = \{(ab, cd) | G(a) = G(b), G(c) \neq G(d), G(c) \neq G(a), G(d) \neq G(a), a, b, c, d \in \mathcal{P}\}$. Γ represents the comparison between an element r_{ab} from diagonal block Σ_{jj} and an element r_{ac} from off-diagonal block Σ_{ij} , sharing a common a . Γ' represents the comparison between an element r_{ab} from diagonal block Σ_{jj} and an element r_{cd} from an off-diagonal block that are not in the same row or column as Σ_{jj} . With Assumption 1, we have $r_{ab} > r_{cd}$, $\forall (ab, cd) \in \Gamma \cup \Gamma'$. We have the following lemma.

LEMMA EC.1. $PCC_{\mathcal{AC}} \geq P\left(\bigcap_{(ab, cd) \in \Gamma \cup \Gamma'} \{\hat{r}_{ab}^n > \hat{r}_{cd}^n\}\right)$, and if all clusters have equal sizes, $PCC_{\mathcal{AC}} \geq P\left(\bigcap_{(ab, ac) \in \Gamma} \{\hat{r}_{ab}^n > \hat{r}_{ac}^n\}\right)$.

This lemma can be proved by induction. In Step 1 of \mathcal{AC} , if event $\bigcap_{(ab, ac) \in \Gamma} \{\hat{r}_{ab}^n > \hat{r}_{ac}^n\}$ occurs, it can be easily verified that two alternatives belonging to the same cluster are merged together. Suppose that at the end of Step $s - 1$, each group contains alternatives from the same cluster. In Step s , assuming A and B represents two groups maximizing the empirical similarity R , they will be merged into one in this step. If event $\bigcap_{(ab, cd) \in \Gamma \cup \Gamma'} \{\hat{r}_{ab}^n > \hat{r}_{cd}^n\}$ occurs, we can prove that A and B must come from the same cluster by contradiction. Assuming A and B do not come from the same cluster: (i) If there are still other groups from the same cluster as A (or B), denoted as A' , then according to $\bigcap_{(ab, ac) \in \Gamma} \{\hat{r}_{ab}^n > \hat{r}_{ac}^n\}$, there exist $a_0 \in A$, $b_0 \in B$ and $a'_0 \in A'$ such that $R(A, B) = \hat{r}_{a_0, b_0}^n < \hat{r}_{a_0, a'_0}^n \leq R(A, A')$, which contradicts the maximization of $R(A, B)$; (ii) If there are no other groups remaining that come from the same cluster as A and B , then, since the algorithm has not yet stopped, there still exist two groups belonging to the same cluster that have not been merged, denoted as C and C' . With $\bigcap_{(ab, cd) \in \Gamma'} \{\hat{r}_{ab}^n > \hat{r}_{cd}^n\}$, we have $R(A, B) < R(C, C')$, which contradicts the maximization of $R(A, B)$. Therefore, A and B must come from the same cluster. Additionally,

if all clusters have the same size, then each cluster's size is known to be $\frac{p}{k}$. In the aforementioned scenario (ii), both group A and B reach maximum size $\frac{p}{k}$. The algorithm will not merge them but will consider the two groups with the second-largest R . Therefore, in this case, correct clustering does not rely on ensuring the occurrence of event $\bigcap_{(ab,cd) \in \Gamma'} \{\hat{r}_{ab}^n > \hat{r}_{cd}^n\}$. Finally, by induction, algorithm \mathcal{AC} stops when only k groups remain, and each group contains alternatives from the same cluster. Therefore, the clustering is correct, and thus, $PCC_{\mathcal{AC}} \geq P\left(\bigcap_{(ab,cd) \in \Gamma \cup \Gamma'} \{\hat{r}_{ab}^n > \hat{r}_{cd}^n\}\right)$. If all clusters have equal sizes, $PCC_{\mathcal{AC}} \geq P\left(\bigcap_{(ab,ac) \in \Gamma} \{\hat{r}_{ab}^n > \hat{r}_{ac}^n\}\right)$.

Following the same proof technique, the convergence of algorithm \mathcal{AC}^+ can be similarly demonstrated. For simplicity, we state without proof that the PCC of \mathcal{AC}^+ is lower bounded by

$$PCC_{\mathcal{AC}^+} \geq P(D)PCC_{\mathcal{AC}}^{(\mathcal{P}_s)} P\left(\bigcap_{(ab,ac) \in \Gamma_q} \{\hat{r}_{ab}^n > \hat{r}_{ac}^n\}\right), \quad (\text{EC.28})$$

where $D \triangleq \bigcap_{j \in \{1, \dots, k\}} \{\sum_{i \in \mathcal{P}_s} \mathbb{I}(G(i) = j) \geq 1\}$ and $PCC_{\mathcal{AC}}^{(\mathcal{P}_s)}$ being the PCC of \mathcal{P}_s by using algorithm \mathcal{AC} . The three terms on the right-hand side of (EC.28) represent the events of “in the support set, there is at least one alternative belonging to \mathcal{G}_j for any $j \in 1, 2, \dots, k$,” “alternatives in the support set are correctly clustered,” and “alternatives in the query set are matched to the correct prototypes”, respectively. If all clusters have equal sizes, the event D can be modeled as the occupancy problem which involves randomly distributing p_s “balls” to k “boxes” (see Example 2.2.10 of Durrett (2019)), and $P(D) \geq 1 - k(1 - 1/k)^{p_s}$. Moreover, with Lemma EC.1, the lower bound of $PCC_{\mathcal{AC}}^{(\mathcal{P}_s)}$ is given by

$$PCC_{\mathcal{AC}}^{(\mathcal{P}_s)} \geq P\left(\bigcap_{(ab,cd) \in \Gamma_s \cup \Gamma'_s} \{\hat{r}_{ab}^n > \hat{r}_{cd}^n\}\right),$$

where $\Gamma_s \triangleq \{(ab, ac) \in \Gamma \mid a, b, c \in \mathcal{P}_s\}$ and $\Gamma'_s \triangleq \{(ab, cd) \in \Gamma' \mid a, b, c, d \in \mathcal{P}_s\}$. If all clusters have equal sizes,

$$PCC_{\mathcal{AC}}^{(\mathcal{P}_s)} \geq P\left(\bigcap_{(ab,ac) \in \Gamma_s} \{\hat{r}_{ab}^n > \hat{r}_{ac}^n\}\right).$$

Next, we will proceed with the specific calculation of $P\left(\bigcap_{(ab,ac)\in\Gamma}\{\hat{r}_{ab}^n > \hat{r}_{ac}^n\}\right)$ and $P\left(\bigcap_{(ab,cd)\in\Gamma'}\{\hat{r}_{ab}^n > \hat{r}_{cd}^n\}\right)$. First, we consider the former, which involves comparing two overlapping correlation coefficients \hat{r}_{ab}^n and \hat{r}_{ac}^n . As shown by Meng et al. (1992), the two overlapping correlations satisfy:

$$\frac{z(\bar{r}_{ab}^n) - z(\bar{r}_{ac}^n) - (z(r_{ab}) - z(r_{ac}))}{\sqrt{\frac{2(1-\bar{r}_{bc}^n)h(a,b,c)}{n-3}}} \sim N(0,1),$$

where $h(a,b,c) = \frac{1-f\cdot\bar{R}^2}{1-\bar{R}^2}$ and $f = \frac{1-\bar{r}_{bc}^n}{2(1-\bar{R}^2)}$, $\bar{R}^2 = \frac{(\bar{r}_{ab}^n)^2 + (\bar{r}_{bc}^n)^2}{2}$. f must be ≤ 1 , and should be set to 1 if $\frac{1-\bar{r}_{bc}^n}{2(1-\bar{r}^2)} > 1$. Then if the assumption “ $r_{ab} \geq r_{ac} + \delta_c$ ” holds for $(ab,ac) \in \Gamma$, we have

$$P(\{\hat{r}_{ab}^n > \hat{r}_{ac}^n\}) \approx P(\bar{r}_{ab}^n > \bar{r}_{ac}^n) = P(z(\bar{r}_{ab}^n) > z(\bar{r}_{ac}^n)) = \Phi\left(\frac{z(r_{ab}) - z(r_{ac})}{\sqrt{\frac{2(1-\bar{r}_{bc}^n)h}{n-3}}}\right) \geq \Phi\left(\frac{\delta_c}{\sqrt{\frac{2(1-\bar{r}_{bc}^n)h}{n-3}}}\right).$$

The “ \approx ” here arises from replacing \hat{r}_{ab}^n with sample correlation coefficient \bar{r}_{ab}^n (the new large-scale estimator (EC.37) is equivalent to the sample correlation as n approaches infinity). Then with Bonferroni lower bound, we have

$$P\left(\bigcap_{(ab,ac)\in\Gamma_\star}\{\hat{r}_{ab}^n > \hat{r}_{ac}^n\}\right) \approx \sum_{(ab,ac)\in\Gamma_\star} \Phi\left(\frac{\delta_c}{\sqrt{\frac{2(1-\bar{r}_{bc}^n)h(a,b,c)}{n-3}}}\right) - (|\Gamma_\star| - 1), \quad (\text{EC.29})$$

where Γ_\star can be Γ , Γ_s or Γ_q . As for $(ab,cd) \in \Gamma'$, r_{ab} and r_{cd} can be approximated as two independent correlations. Then we have (Asuero et al. 2006)

$$\frac{z(\bar{r}_{ab}^n) - z(\bar{r}_{cd}^n) - (z(r_{ab}) - z(r_{cd}))}{\sqrt{\frac{2}{n-3}}} \sim N(0,1).$$

If the assumption “ $r_{ab} \geq r_{cd} + \delta_c$ ” holds for $(ab,cd) \in \Gamma'$, we have

$$P\left(\bigcap_{(ab,cd)\in\Gamma'_\star}\{\hat{r}_{ab}^n > \hat{r}_{cd}^n\}\right) \approx \sum_{(ab,cd)\in\Gamma'_\star} \Phi\left(\frac{\delta_c}{\sqrt{\frac{2}{n-3}}}\right) - (|\Gamma'_\star| - 1) = 1 - |\Gamma'_\star| \left(1 - \Phi\left(\frac{\delta_c}{\sqrt{\frac{2}{n-3}}}\right)\right), \quad (\text{EC.30})$$

where Γ'_\star can be Γ' or Γ'_s .

Finally, with (EC.28), (EC.29) and (EC.30), one can easily calculate the required sample size to achieve a given PCC level. For example, if we want to guarantee that the term $P\left(\bigcap_{(ab,ac)\in\Gamma_q}\{\hat{r}_{ab}^n > \hat{r}_{ac}^n\}\right)$ in equation (EC.28) exceeds α_q , then the required sample size is

$$N(\alpha_q) = \max\left\{0, \left\lfloor \frac{2z^2_{\frac{|\Gamma_q|-\alpha_q}{|\Gamma_q|}}}{\delta_c^2} \max_{(ab,ac)\in\Gamma_q} (1 - \bar{r}_{bc}^{N_0})h(a,b,c) + 3 - N_0 \right\rfloor\right\},$$

where z_α is the α quantile of the standard normal distribution. Similarly, the other terms follow suit.

EC.6. Budget Allocation Policy for Case (a) in Section 6.2.

Let $\Omega \triangleq \mathcal{P} \setminus \{\tau^*\}$, the optimal computing budget allocation is given by:

$$N_i^* = \begin{cases} N_B \left(\sum_{i \in \mathcal{I}^1} \frac{\sigma_i^2}{2\text{cov}(X_{\tau^*}, X_i) - \sigma_{\tau^*}^2 + x_0 N_B (\mu_{\tau^*} - \mu_i)^2} + \sum_{i \in \mathcal{I}^2} \frac{\sigma_i^2 - 2\text{cov}(X_{\tau^*}, X_i)}{x_0 N_B (\mu_{\tau^*} - \mu_i)^2 - \sigma_{\tau^*}^2} + 1 \right)^{-1} & i = \tau^* \\ \frac{\sigma_i^2}{2\text{cov}(X_{\tau^*}, X_i) - \sigma_{\tau^*}^2 + x_0 N_B (\mu_{\tau^*} - \mu_i)^2} N_{\tau^*}^* & i \in \mathcal{I}^1 \\ \frac{\sigma_i^2 - 2\text{cov}(X_{\tau^*}, X_i)}{x_0 N_B (\mu_{\tau^*} - \mu_i)^2 - \sigma_{\tau^*}^2} N_{\tau^*}^* & i \in \mathcal{I}^2 \end{cases} \quad (\text{EC.31})$$

where $x_0 \triangleq \min_{x \in \mathcal{M}(x)} \left(\sum_{i \in \mathcal{I}^1} \frac{\sigma_i^2}{2\text{cov}(X_{\tau^*}, X_i) - \sigma_{\tau^*}^2 + x N_B (\mu_{\tau^*} - \mu_i)^2} + \sum_{i \in \mathcal{I}^2} \frac{\sigma_i^2 - 2\text{cov}(X_{\tau^*}, X_i)}{x N_B (\mu_{\tau^*} - \mu_i)^2 - \sigma_{\tau^*}^2} + 1 \right) x$,

$$\mathcal{I}^2 \triangleq \{i \in \Omega \mid \sigma_i^2 - 2\text{cov}(X_{\tau^*}, X_i) > 0\} \cap \left\{ i \in \Omega \mid \frac{\sigma_{\tau^*}^2 + \sigma_i^2 - 2\text{cov}(X_{\tau^*}, X_i)}{(\mu_{\tau^*} - \mu_i)^2} > x N_B \right\}, \mathcal{I}^1 = \Omega \setminus \mathcal{I}^2,$$

$$\mathcal{M}(x) \triangleq \{x \mid x \geq \max(M_1, M_2)\},$$

$$M_1 = \max_{i: \sigma_i^2 - 2\text{cov}(X_{\tau^*}, X_i) > 0} \frac{\sigma_{\tau^*}^2}{N_B (\mu_{\tau^*} - \mu_i)^2}, \quad M_2 = \max_{i: \sigma_i^2 - 2\text{cov}(X_{\tau^*}, X_i) \leq 0} \frac{\sigma_{\tau^*}^2 + \sigma_i^2 - 2\text{cov}(X_{\tau^*}, X_i)}{N_B (\mu_{\tau^*} - \mu_i)^2}.$$

The derivation and the implementation can be found in Fu et al. (2007). We leave out the technicality that N_i^* may not be an integer. In practice, we need to round it up or down.

EC.7. Proof of Proposition 3.

Proof Taking the derivative of PCS(τ) with respect to N_i , we have

$$\begin{aligned} & \frac{\partial \text{PCS}(\tau)}{\partial N_i} \\ &= \frac{\partial d_i^\tau}{\partial N_i} \int_{-d_1^\tau}^\infty \cdots \int_{-d_{i-1}^\tau}^\infty \int_{-d_{i+1}^\tau}^\infty \cdots \int_{-d_p^\tau}^\infty f_{y^\tau}(y_1, \dots, -d_i^\tau, \dots, y_p) dy_1 \cdots dy_p \\ &+ 2 \sum_{j \in \{1, \dots, p-1\} \setminus \{i\}} \frac{\partial \text{PCS}(\tau)}{\partial \tilde{r}_{i,j}^\tau} \frac{\partial \tilde{r}_{i,j}^\tau}{\partial N_i} \\ &= I'_i + o(I'_i). \end{aligned} \quad (\text{EC.32})$$

The last “=” results from Assumption 2 and Assumption 3. If $N_\tau \geq N_i$, then

$$\frac{\partial d_i^\tau}{\partial N_i} = \frac{\mu_\tau - \mu_i}{2} \cdot \sigma_i^2 \left(\frac{\sigma_\tau^2}{N_\tau} + \frac{\sigma_i^2}{N_i} - 2 \cdot \frac{\text{cov}(X_\tau, X_i)}{N_\tau} \right)^{-\frac{3}{2}} N_i^{-\frac{1}{2}}. \quad (\text{EC.33})$$

If $N_\tau < N_i$, then

$$\frac{\partial d_i^\tau}{\partial N_i} = \frac{\mu_\tau - \mu_i}{2} \cdot \sigma_i \sigma_\tau \left(\frac{\sigma_i}{\sigma_\tau} - 2r_{\tau i} \right) \left(\frac{\sigma_\tau^2}{N_\tau} + \frac{\sigma_i^2}{N_i} - 2 \cdot \frac{\text{cov}(X_\tau, X_i)}{N_i} \right)^{-\frac{3}{2}} N_i^{-\frac{1}{2}}, \quad (\text{EC.34})$$

Therefore, if $N_\tau \geq N_i$ or $r_{\tau i} < \frac{\sigma_i}{2\sigma_\tau}$, $I'_i > 0$ if $\mu_i < \mu_\tau$ and $I'_i < 0$ if $\mu_i > \mu_\tau$.

Next, we will prove that the condition “ $N_{\tau^*} \geq N_i$ ” (for simplicity, referred to as condition \mathcal{N}) will hold for $i \in \mathcal{I}^+(\tau^*)$ in the process of GBA (Algorithm 1) by induction. At the start of the GBA, each alternative is allocated an equal initialization sample size, and thus the condition \mathcal{N} holds. Suppose that the condition \mathcal{N} holds at the iteration step t of GBA. Then, at the step $t+1$, the P-OS is updated from τ_t^* to τ_{t+1}^* . If Assumption 5 holds, as shown in the Figure EC.2, the set $\mathcal{I}^+(\tau^*)$ diminishes monotonically as the iterations proceed. Then we have either $\tau_{t+1}^* = \tau_t^*$ or $\tau_{t+1}^* \in \mathcal{I}^+(\tau_t^*)$.

If $\tau_{t+1}^* = \tau_t^*$, by the allocation policy in Algorithm 1, alternatives in $\mathcal{I}^-(\tau_{t+1}^*) \cup \{\tau_{t+1}^*\}$ will receive non-negative sample sizes and alternatives in $\mathcal{I}^+(\tau_{t+1}^*)$ will receive zero sample. Combing the step t , the condition \mathcal{N} holds.

If $\tau_{t+1}^* \in \mathcal{I}^+(\tau_t^*)$, due to the monotonicity of the diminution of $\mathcal{I}^+(\tau_t^*)$, we have $\mathcal{I}^+(\tau_{t+1}^*) \subseteq \mathcal{I}^+(\tau_t^*) \subseteq \dots \subseteq \mathcal{I}^+(\tau_1^*)$. According to the allocation rule, after the step t is completed, the alternatives in $\mathcal{I}^+(\tau_t^*)$ (including τ_{t+1}^* and $\mathcal{I}^+(\tau_{t+1}^*)$) share the same sample size. Then, at the step $t+1$, alternative τ_{t+1}^* will receive non-negative sample sizes and $\mathcal{I}^+(\tau_{t+1}^*)$ will receive zero sample. The condition \mathcal{N} holds at step $t+1$. By induction, the proof is completed.

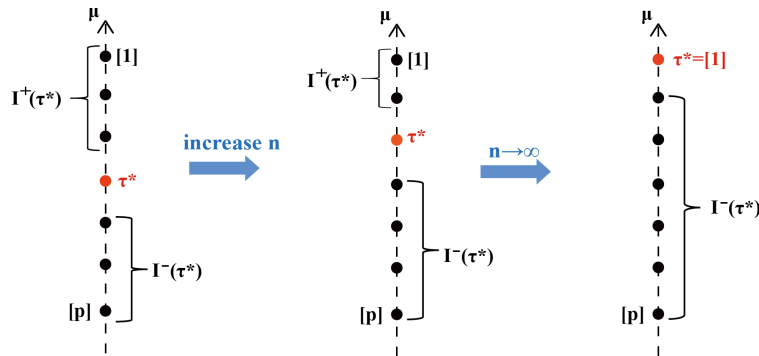


Figure EC.2 As the total sample size increases, the P-OS approaches alternative [1].

EC.8. The Connection between P3C and PCA-based Variable Selection Policy.

Since the behaviors of alternatives are modeled as random variables, a selection policy in R&S can be regarded as a variable selection technique. In this part, we will explain the relationship between PCA-based variable selection strategy in machine learning and P-OS strategy. The terms “variable” and “alternative” refer to the same concept in this part.

Looking into the cluster \mathcal{G}_j , without loss of generality, the alternatives in cluster \mathcal{G}_j are indexed by $\{1, 2, \dots, p_j\}$. By performing PCA to cluster \mathcal{G}_j , we can obtain the first principal component $PC_{\mathcal{G}_j}$, which is defined as a synthetic variable $PC_{\mathcal{G}_j} = k_{1j}X_1 + \dots + k_{p_jj}X_{p_j}$ which maximizes its variance $var(PC_{\mathcal{G}_j})$ subject to $k_{1j}^2 + \dots + k_{p_jj}^2 = 1$. The loading k_{ij} measures the correlation between the alternative i and the principal component. Meanwhile, $PC_{\mathcal{G}_j}$ is the center of this cluster which is proved to be the linear combination that maximizes the sum of squared correlations with the alternatives located in the cluster (Vigneau and Qannari 2003), so it is often used as the *representative* to reflect the information of this cluster. Then the alternative that has the largest loading k_{ij} on the first principal component can serve as the *representative* alternative of this cluster (Al-Kandari and Jolliffe 2001):

$$\tau(\mathcal{G}_j) = \arg \max_{i \in \{1, 2, \dots, p_j\}} k_{ij}. \quad (\text{EC.35})$$

We assume that the behavior of alternatives follows a simple single-factor model. The latent factors of cluster \mathcal{G}_j are merged into one $\zeta_j \sim N(0, \sigma_{\mathcal{G}_j}^2)$, $j = 1, 2, \dots, k$, which are mutually independent. We assume

$$X_i = a_{i, G(i)} \zeta_{G(i)} + \mu_i,$$

where the coefficient a_{ij} quantifies the extent to which the alternative i is affected by the latent factor ζ_j . Then we can state that maximizing k_{ij} is equivalent to maximizing a_{ij} :

$$\tau(\mathcal{G}_j) = \arg \max_{i \in \{1, 2, \dots, p_j\}} a_{ij}. \quad (\text{EC.36})$$

This is because by Cauchy–Schwarz inequality,

$$var(PC_{\mathcal{G}_j}) = (\sum_{i=1}^{p_j} k_{ij} a_{ij})^2 var(\zeta_j) \leq (\sum_{i=1}^{p_j} a_{ij}^2) var(\zeta_j).$$

To make the equality holds, the loading k_{ij} must be proportional to a_{ij} , $i \in \mathcal{G}_j$. According to (EC.36), the PCA-based selection policy $\tau(\mathcal{G}_j)$ maximizes the coefficient with the major latent factor ζ_j of this cluster. It is the most representative alternative that exhibits the largest correlation with other alternatives in this cluster. Nevertheless, its mean μ_τ may be exceedingly small. However, as demonstrated in Chapter 4, the P-OS strategy prioritizes high mean alternatives. Among those with sufficiently high means, P-OS chooses alternatives that have stronger correlations with other alternatives and can better reflect the information of the cluster. Therefore, the PCA-based selection policy is different from P-OS. It is too aggressive for R&S problems as they focus solely on information gain and do not provide any probabilistic guarantee for mean performance. However, when all alternatives have similar mean (i.e., the low-confidence scenario), PCA and P-OS selection policies are consistent, both tending to select the representative alternative that has stronger correlation with other alternatives.

EC.9. The Pseudo-code of Algorithm \mathcal{AC} and \mathcal{AC}^+ .

The pseudo-codes of \mathcal{AC} and \mathcal{AC}^+ are provided in the Algorithm 2 and Algorithm 3, respectively.

Algorithm 2 Linkage Alternative Clustering (\mathcal{AC})

Input: estimated covariance matrix $\hat{\Sigma}_n$, the number of clusters k

Initialization: Compute estimated correlation coefficient r_{ab} , $a, b \in \mathcal{P}$ from covariance matrix $\hat{\Sigma}_n$. Initialize the collection of clusters \mathcal{C} as $\{\{1\}, \dots, \{p\}\}$ and the number of clusters $N_{\mathcal{C}}$ as p .

While $N_{\mathcal{C}} > k$ **do**

(i) Compute R_{XY} for each cluster pair $(X, Y) \in \mathcal{C}$. (ii) Solve $(A, B) = \arg \max_{(X, Y) \in \mathcal{C}} R_{XY}$. (iii) Let $M(A, B) = \{i | i \in A \cup B\}$. (iv) $\mathcal{C} \leftarrow \mathcal{C} - A - B + M(A, B)$. (v) $N_{\mathcal{C}} \leftarrow N_{\mathcal{C}} - 1$.

end while

Return the partition \mathcal{C} and label the clusters in \mathcal{C} with index $1, 2, \dots, k$.

Algorithm 3 Few-shot Alternative Clustering \mathcal{AC}^+

Input: sample size n , the number of clusters k , p_s, p_q .

Step 1: Randomly split the set \mathcal{P} into two sets, \mathcal{P}_s and \mathcal{P}_q , with sizes p_s and p_q , respectively.

Step 2 (Selecting Prototypes): On a single processor, simulate n samples for each alternative in \mathcal{P}_s and calculate the estimated covariance matrix $\hat{\Sigma}_n^{\mathcal{P}_s}$ with (EC.37). Input $\hat{\Sigma}_n^{\mathcal{P}_s}$ into the algorithm \mathcal{AC} and output the clustering result $\Pi_n^{\mathcal{P}_s}$. Within \mathcal{P}_s , calculate the *prototype* τ_j of cluster \mathcal{G}_j with (5), $\forall j \in \{1, 2, \dots, k\}$. Let $\mathcal{P}_p = \{\tau_1, \dots, \tau_k\}$.

Step 3 (Matching): Send a copy of \mathcal{P}_p to each processor. Randomly and equally allocate \mathcal{P}_q to each processor. For any $j \in \mathcal{P}_q$, simulate alternative j for n times and calculate $\hat{r}_{\tau_i, j}^n$ for any $i \in \{1, 2, \dots, k\}$. $G_n(j) = \arg \max_{i \in \{1, 2, \dots, k\}} \hat{r}_{\tau_i, j}^n$.

Return the partition Π_n .

EC.10. Large-dimensional Covariance Matrix Estimator

We adopt the naive Equal Allocation (EA) policy for covariance estimation. The reason is that by using EA, we simulate the complete vector (X_1, X_2, \dots, X_p) at one time, generating a complete data matrix $\mathcal{X}_n^T = (x_{ij}) \in \mathbb{R}^{p \times n}$ after sampling n times. Otherwise, if the sample sizes are unequal, it becomes a statistically challenging problem known as ‘‘covariance estimation with missing data’’ (Pavez and Ortega 2020, Gorder and Kolonko 2019).

In large-scale situation, the traditional estimator is given by $S_n = \frac{\tilde{\mathcal{X}}_n^T \tilde{\mathcal{X}}_n}{n-1}$, where $\tilde{\mathcal{X}}_n$ is obtained from \mathcal{X}_n by subtracting the mean of each column. The analytical nonlinear shrinkage estimator (Ledoit and Wolf 2020), originally from the study of the spectral distribution of quantum energy levels in physics, is given by

$$\hat{\Sigma}_n = \sum_{i=1}^p \hat{\lambda}_{n,i} \cdot u_{n,i} u_{n,i}^T, \quad (\text{EC.37})$$

where

$$\hat{\lambda}_{n,i} = \frac{\lambda_{n,i}}{[\pi_n^{\frac{p}{2}} \lambda_{n,i} f_n(\lambda_{n,i})]^2 + [1 - \frac{p}{n} - \pi_n^{\frac{p}{2}} \lambda_{n,i} \mathcal{H}(\lambda_{n,i})]^2},$$

$$f_n(\lambda_{n,i}) = \frac{1}{p} \sum_{j=1}^p \frac{3}{4\sqrt{5}\lambda_{n,j} n^{-\frac{1}{3}}} \left[1 - \frac{1}{5} \left(\frac{\lambda_{n,i} - \lambda_{n,j}}{\lambda_{n,j} n^{-\frac{1}{3}}} \right)^2 \right]^+,$$

$$\mathcal{H}(\lambda_{n,i}) = \frac{1}{p} \sum_{j=1}^p \left\{ -\frac{3(\lambda_{n,i} - \lambda_{n,j})}{10\pi\lambda_{n,j}^2 n^{-\frac{2}{3}}} + \frac{3 \left[1 - \frac{1}{5} \left(\frac{\lambda_{n,i} - \lambda_{n,j}}{\lambda_{n,j} n^{-\frac{1}{3}}} \right)^2 \right]}{4\sqrt{5}\pi\lambda_{n,j} n^{-\frac{1}{3}}} \cdot \log \left| \frac{\sqrt{5}\lambda_{n,j} n^{-\frac{1}{3}} - \lambda_{n,i} + \lambda_{n,j}}{\sqrt{5}\lambda_{n,j} n^{-\frac{1}{3}} + \lambda_{n,i} - \lambda_{n,j}} \right| \right\}.$$

$\lambda_{n,i}$ ($i = 1, 2, \dots, p$) is the eigenvalue of S_n and $u_{n,i}$ is the corresponding eigenvector, which are obtained by performing matrix spectral decomposition on S_n . Notably, as n approaches infinity with a fixed p , the $\hat{\Sigma}_n$ will approach the sample covariance matrix S_n . This estimator has closed-form, which only requires matrix decomposition of S_n one time.

References in Online Appendices

- Al-Kandari NM, Jolliffe IT (2001) Variable selection and interpretation of covariance principal components. *Communications in Statistics-Simulation and Computation* 30(2):339–354.
- Asuero AG, Sayago A, González AG (2006) The correlation coefficient: An overview. *Critical Reviews in Analytical Chemistry* 36:41 – 59, URL <https://api.semanticscholar.org/CorpusID:39213560>.
- Azaïs JM, Wschebor M (2009) *Level sets and extrema of random processes and fields* (John Wiley & Sons).
- Durrett R (2019) *Probability: theory and examples*, volume 49 (Cambridge university press).
- Fu MC, Hu JQ, Chen CH, Xiong X (2007) Simulation allocation for determining the best design in the presence of correlated sampling. *INFORMS Journal on Computing* 19(1):101–111.
- Görder B, Kolonko M (2019) Ranking and selection: A new sequential bayesian procedure for use with common random numbers. *ACM Transactions on Modeling and Computer Simulation (TOMACS)* 29(1):1–24.
- Hashorva E, Hüsler J (2003) On multivariate gaussian tails. *Annals of the Institute of Statistical Mathematics* 55:507–522.
- Ledoit O, Wolf M (2020) Analytical nonlinear shrinkage of large-dimensional covariance matrices .
- Meng XL, Rosenthal R, Rubin DB (1992) Comparing correlated correlation coefficients. *Psychological bulletin* 111(1):172.
- Pavez E, Ortega A (2020) Covariance matrix estimation with non uniform and data dependent missing observations. *IEEE Transactions on Information Theory* 67(2):1201–1215.

Vigneau E, Qannari E (2003) Clustering of variables around latent components. *Communications in Statistics-Simulation and Computation* 32(4):1131–1150.